MAX-PLANCK-INSTITUT FÜR PLASMAPHYSIK

GARCHING BEI MÜNCHEN

Radiative Thermal Instability and Bifurcation

P. Bachmann, D. Sünder

Max-Planck-Institut für Plasmaphysik Garching,
Association EURATOM, Division Berlin, Mohrenstr. 40-41,
D-10117 Berlin, Germany

July 26, 1994

IPP 8/4 July 1994

Die nachstehende Arbeit wurde im Rahmen des Vertrages zwischen dem Max-Planck-Institut für Plasmaphysik und der Europäischen Atomgemeinschaft über die Zusammenarbeit auf dem Gebiete der Plasmaphysik durchgeführt.

Abstract

A radial hydrodynamic model is used to investigate the radiative thermal instability in the scrape-off layer by applying a linear stability analysis of existing equilibrium states. Phase space trajectories are analyzed to derive conditions of their existence and bifurcation. Equilibrium profiles are calculated for the cases of homogeneous plasma temperature, plasma density and self-consistency. Unstable perturbations, localized in the scrape-off layer, may lead to a strongly radiating detached plasma belt.

Contents

1 Introduction

The global stability and confinement of a tokamak plasma are significantly influenced by the boundary plasma parameters. The onset of density disruptions, which limit the maximum plasma density, is triggered by impurity radiation in the edge plasma [1], [2]. Increasing the electron density increases energy loss in the boundary, where radiative cooling is an essential loss mechanism. If the plasma density reaches a threshold, the radiative condensation thermal instability is excited and a poloidally asymmetric Marfe appears [3] - [6]. After a time of about 100 ms the Marfe decays and the radiation comes from a poloidally symmetric shell around the plasma edge [1]. Above a second density threshold the temperature in the SOL decreases due to the onset of the radiative thermal instability (RTI). This detached plasma state is unstable to magnetic perturbations, and after a series of small disruptions the tokamak discharge undergoes a terminal disruption. The RTI was first analyzed in the frame of a simple model in [3]. As the only loss mechanism, this model considers radiation described by a step function profile, neglecting the effects of neutral particles and limiter losses. When the radiation loss is equal to the input power, the equilibrium state is marginally stable. A model which considers the neutral particle dynamics more correctly was first presented in [7].

In this paper a one-dimensional model [8] is used to investigate the effect of neutral particles, of heating and loss processes on the plasma equilibrium state with respect to the existence of critical parameters and the RTI in SOL plasmas. The dynamics of the plasma and neutral particles is described by a consistent set of hydrodynamic equations averaged along the magnetic field lines. Ionization, charge exchange, plasma particle and energy losses to the limiter, neutral particle recycling at the limiter and radiative cooling of the edge plasma by carbon impurity ions are taken into consideration (see section 2).

The stationary problem is investigated in section 3. The goal is to compute profiles of densities, temperature and their fluxes for existing equilibrium states. An existence theorem is formulated which implies that existence domains in the phase space are limited by quasi-singular points that are characterized by critical quantities (section 3.1). Existence conditions for equilibrium states are investigated by analyzing phase space trajectories, and profiles are calculated, both in different approaches: homogeneous temperature (sect. 3.2), homogeneous density (sect. 3.3), linearized solution (sect. 3.4), numerical solution (sect. 3.5). A change of the parameters of the system may lead to bifurcation which is the essential mechanism that disrupts existing equilbrium states.

The RTI is studied in section 4 by applying a linear stability analysis. Linearizing the MHD equations, we find unstable perturbations, localized in the SOL, which lead to a strongly radiating detached plasma belt. The effect of the energy input and the limiter losses on the RTI are discussed.

2 Model Equations

Averaging the MHD equations over the magnetic field lines and taking into account the boundary conditions at the limiter plates $z = 0$ and $z = L$,

$$\begin{aligned} v(z=0) = -v_s, \quad v(z=L) = v_s, \\ \Gamma_{N\|}(z=0) = Rnv_s, \Gamma_{N\|}(z=L) = -Rnv_s, \\ \Gamma_{T\|}(z=0) = -\delta_T nv_s T, \Gamma_{T\|}(z=L) = \delta_T nv_s T, \end{aligned} \tag{1}$$

we describe the motion of the plasma and neutral particles perpendicular to the magnetic field by

$$\partial_t n + \partial_x \Gamma_{n\perp} = k_i(T)nN - \theta n/\tau_1(T), \tag{2}$$

$$\partial_t N + \partial_x \Gamma_{N\perp} = -k_i(T)nN + \theta Rn/\tau_1(T), \tag{3}$$

$$\partial_t 3nT + \partial_x \Gamma_{T\perp} = H(T) - Q_R(T, \xi_N) - k_i(T)nNR_y - \theta nT/\tau_2(T), \tag{4}$$

$$\Gamma_{n\perp} = -D_\perp(n,T)\partial_x n, \ \Gamma_{N\perp} = -\frac{1}{2k_{cx}n}\partial_x v_s^2 N, \ \Gamma_{T\perp} = -\kappa_\perp(n,T)\partial_x T, \tag{5}$$

$H(T) := \sigma(T)E^2$, where x and z are the coordinates perpendicular and parallel to the magnetic field, $v, \Gamma_{N\|}, \Gamma_{T\|}$ and $v_s = \sqrt{2T/m_i}$ are the plasma velocity, neutral particle flux, the heat flux of the plasma parallel to the magnetic field, and ion sound velocity, respectively; R is the recycling coefficient at the limiter and $\delta_T \simeq 4$; n, $(\Gamma_{n\perp})$, T, $(\Gamma_{T\perp})$, N, $(\Gamma_{N\perp})$ are the plasma density, plasma temperature, neutral particle density with their respective perpendicular anomalous fluxes included in parentheses; $D_\perp$ and $\kappa_\perp$ are the coefficients of the perpendicular anomalous plasma diffusion and heat conduction, $\sigma = \sigma_0 T^{3/2}$ is the classical electrical conductivity; k_i and k_{cx} are the rate coefficients for ionization and charge exchange and E is the toroidalelectric field of the tokamak; $R_y = 13.6eV$. $\tau_m := \beta_m L/v_s$ is the lifetime of the plasma ($m = 1$) in the SOL and its energy ($m = 2$) due to streaming along the field lines to the limiter ($\beta_1 = 1/2, \beta_2 = 1/2\delta_T$, L - connection length); $x := r - r_s$, r_s is the separatrix radius, and $\theta \equiv \theta(x)$ is the Heaviside function. $\partial_{t,x}$ denote the partial derivates with respect to t, x.

For the cooling rate Q_R we use the analytical expression of [7], [13] which takes especially charge exchange processes between carbon ions and atomic hydrogen into consideration:

$$Q_R := n^2 \xi_i \ G(T, \xi_i) \ [W/cm^3], \tag{6}$$

$$\begin{aligned} G = A(T - T_1)e^{-B(T-T_1)}, \\ A = 10^{-26}(3.1e^{-0.024(ln\xi_N+11)^2} + 0.7), \ B = 0.6e^{-7.810^{-4}(ln\xi_N+14)^{3.4}} + 0.055 \end{aligned} \tag{7}$$

T in eV with $5\ eV \leq T \leq 50\ eV$, n in cm^{-3}, $T_1 = 4.4eV, \xi_i = n_c/n$, where n_c is the mean carbon ion density.

We introduce the 6-dimensional vector function $\vec{y}(x,t)$ which is composed by subsequent pairs of scalars A followed by their respective fluxes Γ_A (in the following "$\perp$" will be omitted) for $A = n, T, N$:

$$\vec{y} := (n, \Gamma_n, T, \Gamma_T, N, \Gamma_N)^T , \tag{8}$$

The system of equations (2)-(4) can then be written in vector notation as

$$\left(\hat{A}\partial_t + \hat{E}\partial_x\right) \cdot \vec{y} = \vec{f}, \tag{9}$$

where $\hat{A}(\vec{y})$ is a 6×6 matrix function with the only non-vanishing elements $A_{11} = A_{25} = 1, A_{31} = 3y_3, A_{33} = 3y_1$, and $\hat{E}$ is the identity matrix. The vector function $\vec{f}(x, \vec{y})$ contains the remaining rhs terms of eqs. (2) - (4). We consider initial value problems (IVP) and boundary value problems (BVP) to eq. (9) which represents a system of non-linear first-order partial differential equations.

3 Equilibrium: Critical Parameters and Bifurcation

3.1 General

We investigate steady-state solutions ($\partial_t = 0$) to the system of equations (9) on the domain $X = [x_c, x_w]$ (x_c - position in the central plasma, x_w - distance from the separatrix, located at $x = 0$, to the wall) which results in the equation

$$\partial_x \vec{y} = \vec{f} \tag{10}$$

to be solved. The equations for the fluxes Γ_A (5) are balance equations

$$\partial_x \Gamma_A = H_A - L_A \tag{11}$$

with source (H_A) and loss (L_A) terms, which can be integrated formally:

$$\Gamma_A^2(x) = \Gamma_{A0}^2 + 2\int_{x_0}^{x} dx' \, \Gamma_A (H_A - L_A). \tag{12}$$

Scalars and fluxes at a position x_0 are denoted by $A_0 := A(x_0), \Gamma_{A0} := \Gamma_A(x_0)$. Our treatment can be simplified as follows. For the case both of complete recycling at the limiter ($R = 1$) and at the wall,

$$\Gamma_n + \Gamma_N = 0, \tag{13}$$

the system of equations (10) contains a first integral

$$N\,T = c - \alpha n^2 \tag{14}$$

with $\alpha := m_i k_{cx} D/2$ and the constant c which is determined by initial or boundary conditions. Thus the neutrals can be completely eliminated from our treatment, i.e. the

number of variables can be reduced to only 4 variables ($A \rightarrow n, T$), and the boundary value of the neutral particle density can be considered as a parameter.

We consider IVP and BVP to eq. (10). Suppose that the function $\vec{f}$ and the Jacobian matrix $\hat{J}_f := \partial\vec{f}/\partial\vec{y}$ are continous on X. Then there exists a unique solution of the IVP for (11) which can be constructed by means of Euler polygons. The goal of this treatment is to calculate profiles $\vec{y}(x)$ of existing equilibrium states for BVP. To ensure uniqueness for the solution of BVP, one can make use of the property of the system (10) to be *quasi-monotonically* [9], [10]. To find conditions under which equilibrium states exist, we start with an *existence theorem* [7]: An equilibrium state exists if the following inequalities are fulfilled:

$$\Gamma_A^2 \geq 0, \quad A \geq 0 \quad \forall\, x \in X. \tag{15}$$

These conditions restrict physically possible solution manifolds to be contained in limited existence domains in the phase space $S := \{\vec{y}\}$. We analyze phase space trajectories in S in order to derive existence conditions for the parameters of the system (10) $\vec{p} \in P$ (P is the parameter space) which should also contain remaining boundary values.

A point $\vec{y}_0 \in S$ is said to be *quasi-singular* if it is an element of the hypersurface $S_i := \{\vec{y} \mid f_i = 0\} \subseteq S$, where f_i is the ith component of $\vec{f}$. The cases of equality in (15) are related to conditions $f_i = 0$. We define $S^{(6-m)} := \bigcap_i^{(m)} S_i$ where m is the total number of the hypersurfaces S_i. If $m = 6$, $S^{(0)}$ is identical with the *singular point*:

$$\vec{y}_0 = \vec{y}^0 \equiv S^{(0)}, \quad \vec{f}(\vec{y}^0) = 0. \tag{16}$$

The reason to introduce the concept of quasi-singularity is that quasi-singular points limit existence domains in S . Therefore, we have especially to analyze phase space portraits in the vicinity of quasi-singular points and look for conditions under which these portraits are changed when the parameter vector $\vec{p}$ is changed. Consider, for instance, a contineous change of the $\vec{p}$ along a curve C_p in P. When the phase space portrait gets restructured qualitatively in passing through certain points on C_p, these points are called its *bifurcation points*, while the associated parameter values $\vec{p}*$ *bifurcation values* [11]. Because this analysis is a complicated task, we consider simplified cases in the next sections.

The conditions (14) suggest that (A, Γ_A^2) phase space representations be considered. We investigate IVP for the two domains $x < 0$ (I) and $x > 0$ (II) separately. We focus our attention on the second domain (SOL), because the first one is a special case of it. Before presenting numerically calculated profiles for the whole domain X in sect. 3.5, we consider special cases in sects. 3.2 - 3.4. As far as possible, we apply analytical methods and consider also solutions on the domain $X_0 := (-\infty, \infty) \supseteq X$. *Bifurcation* turns out to be the essential mechanism to disrupt equilibrium states with changing parameter $\vec{p}$. Let us emphasize that our analysis is restricted up to now to the spatial equilibrium problem only (to the temporal problem see sect. 4).

3.2 Homogenous temperature

For the case that T is assumed to be homogenous, eq. (11) can easily be integrated, starting at the lhs of each domain (finite central position x_c, separatrix at $x_s = 0$):

$$\tilde{\Gamma}_n^2 \;=\; (n^2 - \mu)^2 \;-\; \Delta, \tag{17}$$

$$\mu := \begin{cases} \mu_I := c/\alpha & \text{for } x < 0 \text{ (I)} \\ \mu_{II} := \tilde{c}/\alpha & \text{for } x > 0 \text{ (II)}, \end{cases} \tag{18}$$

$$\Delta := \begin{cases} \Delta_I := (n_c^2 - \mu)^2 - \tilde{\Gamma}_{nc}^2 & \text{for } x < 0 \text{ (I)} \\ \Delta_{II} := (n_s^2 - \mu)^2 - \tilde{\Gamma}_{ns}^2 & \text{for } x > 0 \text{ (II)}, \end{cases} \tag{19}$$

$\tilde{c} := c - T/(k_i\tau), \tilde{\Gamma}_n := \Gamma_n/\sqrt{D\alpha k_i/2T}$.

Replacing x by $\tilde{x} := x\sqrt{D\alpha k_i/2T}/D$, one can integrate $\tilde{\Gamma}_n = -dn/d\tilde{x}$ by means of eq. (17) with the result that $\tilde{x}$ as a function of n can be expressed analytically in terms of the elliptic integral of the first kind $F(\phi, m)$:

$$\tilde{x}(n) = -\int^n dn' \,/\tilde{\Gamma}(n') \;=$$

$$\frac{1}{\sqrt{\mu - \sqrt{\Delta}}}\, F\left[arcsin\left(\frac{n}{\sqrt{\mu + \sqrt{\Delta}}}\right), \frac{\mu + \sqrt{\Delta}}{\mu - \sqrt{\Delta}}\right]. \tag{20}$$

The inverse function $n(\tilde{x})$ can be expressed by the elliptic Jacobi function $sn\left(\sqrt{\mu - \sqrt{\Delta}}\tilde{x}, m\right)$ with the quarter-period $K(m) = F\left(\frac{\pi}{2}, m\right)$.

As phase space representation we consider $\tilde{\Gamma}_n^2$ as a function of n^2 in dependence of the parameters $\mu, \tilde{\Gamma}_{n(c,s)}$ according to eqs. (17) - (19). The quantities used in the discussion are *normalized* as follows:

$$x \to \tilde{x}, \Gamma_{n(c,s)} \to \tilde{\Gamma}_{n(c,s)}/n_{c,s}^2, n \to n/n_{c,s}, \mu \to \mu/n_{c,s}^2, \Delta \to \Delta/n_{c,s}^2. \tag{21}$$

Γ_n^2 has a minimum at the point $(\mu, -\Delta)$ which is below the n^2 axis if $\Delta > 0$. The function Γ_n^2 then has the two roots $n_{1,2}^2 = \mu \pm \sqrt{\Delta}$. Fig. 1, where this dependence is displayed for the domain I for different parameters μ_I (which are always positive) and Γ_{nc}, shows that in the region $0 \leq n^2 \leq 1$ equilibrium states always exist. This means that for an arbitrary parameter μ_I each value of the density at the separatrix can be realized with suitably chosen initial values with the particle flux following from eq. (17). These values will be used as the initial values for domain II. Density profiles for domain I calculated by means of eq. (20) are shown in Fig. 2 for vanishing neutral particle density and different particle fluxes Γ_{nc}. For the case $\Gamma_{nc} = 0$ ($\Delta_I = 0,\ m = 1,\ x_c = -\infty$) we obtain the analytic solution

$$n \;=\; th\left[\sqrt{\mu_1}\,(a_1 - x)\right] \;,\; a_1 \;=\; \frac{arcth\; n_s}{\sqrt{\mu_I}}. \tag{22}$$

The phase space representation for domain II (SOL) is shown in Fig. 3 for $\Gamma_{ns} = 1$ and for parameters $\mu = -1...1$ which may change from negative to positive values. An equilibrium state exists for the case that $\Delta < 0$. For $\Delta > 0$ existence conditions become more complicated. In order to investigate them, we proceed to analyze the parameter space with respect to existence. The two remaining parameters μ, Γ_{ns} are displayed in Fig. 4. Above the curve $\Delta = 0$ there is existence for $0 \leq n^2 \leq 1$. For $\Delta > 0$ there are also possible phase trajectories for $n_1^2 \leq n^2 \leq 1$, where $n_1^2 = \mu + \sqrt{\Delta}$ is the larger of the two zeros (see Fig. 3). The existence domain becomes larger and is extended to areas above the curves where n_1^2 becomes equal to a certain value c_0 (Fig. 4). In the sense of the definition introduced in the foregoing section, $\Delta = 0$, $n_1^2 = c_0$ can be understood as bifurcation lines that divide the parameter subspace into an existing and non-existing region. Phase trajectories may thus exist from $n^2 = 1$ to c_0 where $\Gamma_n^2 = 0$ with a curve parameter $x = x_{10}$ which follows from eq. (20):

$$x_{10}(\mu, \Gamma_{ns}^2) \;=\; x(\sqrt{c_0}) \;- x(1). \tag{23}$$

This means that for a given parameter there is a maximum extension x_{10} of the SOL such that an equilibrium state does not exist for $x_w > x_{10}$. This is demonstrated in Fig. 5, where contour plots $x_1(\mu, \Gamma_{ns}^2) = x_{10}$ for different x_{10} values are displayed. The existence region is above the given curve. x_1 as a function of the parameters is shown in Fig. 6. The used parameter subspace is divided into existing and nonexisting regions by a bifurcation surface. Density profiles that realize existence are shown in Fig. 7. Special analytical solutions exist for the case $x\left(\sqrt{c_0}\right) = \infty$, which is connected with $K = \infty, (m = 1)$ of the elliptic Jacobi function:

$$n \;=\; \frac{\sqrt{2|\mu_{II}|}}{sh\left[\sqrt{2|\mu_{II}|}\,(x + a_2)\right]},\; a_2 \;=\; \frac{arcsh\sqrt{2|\mu_{II}|}}{\sqrt{2|\mu_{II}|}} \tag{24}$$

for $\mu_{II} < 0$ and

$$n \;=\; \sqrt{\mu_{II}}cth\left[\sqrt{\mu_{II}}\,(x + a_3)\right],\; a_3 \;=\; \frac{arccth\left(\frac{1}{\sqrt{\mu_{II}}}\right)}{\sqrt{\mu_{II}}} \tag{25}$$

for $\mu_{II} > 0$, where n_s, needed for the coupling with the solution for domain I, must be determined for eqs. (24) and (25) from the relations $\Delta_{II}(n_s) = \mu_{II}^2$ and $\Delta_{II}(n_s) = 0$, respectively.

Finally, let us consider how the neutrals act. Eq. (14) shows that c increases with increasing neutral particle density. With otherwise constant parameters, an increase of μ may lead to arriving at the boundary of existence with susequent bifurcation (see Figs. 4, 5). Thus, the neutrals force bifurcation and, in this sense, they destabilize existing equilibrium states.

3.3 Homogeneous plasma density

Next n is considered as a constant parameter. Integrating (11) yields

$$\Gamma_T^2 = C - 2\kappa \left[\frac{5}{2} \left(\beta_0 - \theta \frac{n}{\tau_0} \right) T^{5/2} - c_N n R_y S_i(T) - \xi_i n^2 S_r(T, \xi_N) \right] \tag{26}$$

with $\beta := \sigma_0 E^2$, $\tau_0 := \beta_2 L \sqrt{m/2}$, C being an integration constant determined by the boundary conditions, and $c_N := c - \alpha n^2$. The functions $S_{i,r}$, describing ionization and radiation losses, respectively, are given by the following expressions, which can subsequently be approximated:

$$S_i(T) := \int dT \, \frac{k_i(T)}{T} \cong 2 k_{i0} R_y \left[\sqrt{\frac{T}{R_y}} exp(-R_y/T) + \pi \; erf \left(\sqrt{\frac{R_y}{T}} \right) \right], \tag{27}$$

$$S_r(T, \xi_N) := \int dT \; Q(T, \xi_N) \cong -\frac{A}{B^2} [1 + B(T - T_1)] \, exp[-B(T - T_1). \tag{28}$$

$erf(x)$ denotes the error function. These approximations presuppose the following simplifying assumptions to be valid:

$$k_i(T) \; = \; k_{i0} \sqrt{\frac{T}{R_y}} exp(-R_y/T), \;\; \xi_N \; = \; const \tag{29}$$

with $k_{i0} = 0.73 \times 10^{-8} cm^3/s$. To discuss possible equilibrium states, we focus our attention on the SOL domain by assuming the initial values at the separatrix T_s, Γ_{Ts} to be given. The integration constant C in eq. (27) is then determined by the condition $\Gamma_T(T_s) = \Gamma_{Ts}$:

$$C = \Gamma_{T_s}^2 + 2\kappa \left[\frac{5}{2} \left(\beta_0 - \frac{n}{\tau_0} \right) T_s^{5/2} - c_N n R_y S_i(T_s) - \xi_i n^2 S_r(T_s, \xi_N|_{T=T_s}) \right] \tag{30}$$

Integrating $\Gamma_T = -\kappa dT/dx$ leads to

$$x(T) = -\kappa \int^T dT' \; / \Gamma_T(T'). \tag{31}$$

In the following, we use the *normalized* quantities

$$n, \; N \rightarrow \frac{n, \; N}{10^{12}/cm^3}, T \rightarrow \frac{T}{eV}, k_i \rightarrow \frac{k_i}{cm^3 s^{-1}}, L \rightarrow \frac{L}{cm}, \Gamma_T \rightarrow \frac{\Gamma_T}{(MW/10^6 cm^2)}, \tag{32}$$

and the parameters $\kappa = nD$, $D = 10^4 cm^2/s$, $\xi_i = 0.1$, $\beta_0 = 0$.

Figs. 8 a, b show phase space representations (T, Γ_T^2) for the initial values at the separatrix, $T_s = 50$, $\Gamma_{Ts} = 1$ and $L = 3500$, with the plasma density n as parameter for two different separatrix densities of the neutrals, $N_s = 10^{-4}$ (Fig. 8a) and $N_s = 10^{-2}$ (Fig. 8b). As already pointed out for the case of constant temperature, the neutrals destabilize existing equilibrium states. For the last (dotted) curve of Fig. 8b we show in Fig. 9 how the different loss processes contribute to the total one. Over the whole scrape-off layer the

ionization loss is negligible. For low temperatures the radiation loss becomes comparable to the energy loss due to free streaming along the field lines, but for temperatures below 16 eV no equilibrium state exists.

To estimate existence criteria, the situation here is similar to that of sect. 3.2: Figs. 8a, b show that there are possible equilibrium states for temperatures below the temperature at the separatrix until the existence conditions (14) do not hold any more. Considering for otherwise fixed parameters the dependence on the plasma density n, there is a critical density n_1 with the zero $T_1(n_1) = 0$ such that there is no equilibrium state for densities above it (compare Figs. 8 with Fig. 3). This also limits the extension of the scrape-off layer to down to a critical one (cp. eq. (23)).

Fig. 10 shows the existence diagram (n, T), where the zeros $T_1(n)$ for different separatrix densities are plotted. For neutral particle densities larger than 10^{-2} the lowest temperature of 5 eV cannot be attained. With increasing neutral particle density at the separatrix, the existing domain, which is above the respective curve, is diminished. Fig. 11 shows temperature profiles for $N_s = 10^{-4}$ with different n for parameters that allow the temperature of 5 eV to be attained (the remaining parameters are those of Fig. 10).

3.4 Linearized solution

In the foregoing sections phase space representations on the hypersurfaces $T = const, n = const$ were studied. Here we apply the qualitative theory of dynamical systems by analyzing phase trajectories in the vicinity of singular solutions (see e.g. [12]) for equilibrium states. This restricts the variety of IVP and BVP to those whose phase space trajectories attain singular points. But bifurcation becomes more clearly.

Introducing the variable $\vec{\xi} := \vec{y} - \vec{y}_0$ we linearize eq. (10) in a vicinity of $\vec{y}_0$:

$$\partial_x \vec{\xi} \;=\; \hat{J}_f(\vec{y}_0) \cdot \vec{\xi}, \tag{33}$$

where $\hat{J}_f := \partial \vec{f} / \partial \vec{y}$ is the Jacobian matrix of the system (10). This equation can be used to investigate phase portraits in the vicinity of $\vec{y}_0$. We consider the simplest case, when this point is the singular point of eq. (10), $\vec{y}_0 = \vec{y}^0$ (16). Then (33) represents a homogeneous system of linear differential equations with constant coefficients that can easily be solved with the ansatz $\vec{\xi} \sim exp(\lambda x)$. The eigenvalues λ_i are the roots of the characteristic equation

$$det\ (\hat{J}_f \;-\; \lambda \hat{E}) \;=\; 0, \tag{34}$$

where *det* denotes the determinant.

The solution of the equation for the singular points (16) results in

$$\Gamma_n^0 = 0,\ \Gamma_T^0 = 0,\ n^0 = 0,\ H(T^0) = 0. \tag{35}$$

We obtain four roots of the characteristic equation (34) which are different from 0:

$$\lambda_{1,2} = \pm\sqrt{-c_1/D} \tag{36}$$

with

$$c_1 := k_i(T^0)N^0 - 1/\tau_1(T^0) \tag{37}$$

and

$$\lambda_{3,4} = \pm\sqrt{-c_2/\kappa} \tag{38}$$

with $c_2 := \partial H/\partial T|_{T=T^0}$. N^0 is determined by eq. (14). If we assume $c_2 = 0$, the remaining eigenvalues (36) are either real (a) ($c_1 < 0$) or imaginary (b) ($c_1 > 0$) with different sign. For the first case (a) the phase portrait for $(n, \partial_x n)$ is a saddle point, for the latter (b) it is a vortex. The phase portrait is changed from a saddle point to a vortex for

$$c_1 = 0 \;\Leftrightarrow\; k_i(T^0)\tau_1(T^0)N^0 = 1. \tag{39}$$

This results in a condition for the constant c. Any change of the parameter vector $\vec{p}$ passing through the surface $c_1 = 0$ restructs qualitatively the phase portrait, i.e. bifurcation occurs. As mentioned above, this point in the parameter space is called the bifurcation point with the associated bifurcation values $\vec{p}*$. Only for the first case (a) BVP can be solvable. If there are no neutrals only the first case (a) appears, i.e. the neutrals act destabilizing which is again the above obtained result. To relate this result with that of sect. 3.2, leads to $\Delta_{II} = \mu_{II}^2, \mu_{II} = c_1 k_i(T_0)/(\alpha T_0)$. So bifurcation occurs at $\mu_{II} = 0$ which is identical with $\Delta_{II} = 0$.

3.5 Numerical results

The analysises of the foregoing sections are the starting point for studying the numerical solution of BVP to the system of equations (10). For the numerical solution we consider the whole domain $X = [x_c, x_w]$ without dividing it into two parts. So the rhs $\vec{f}$ becomes x-dependent. We suppose that the boundary conditions are of the form: fluxes Γ_A given left (at $x = x_c$), scalars A given right (at $x = x_w$):

$$\Gamma_n(x_c) = \Gamma_{nc},\ \Gamma_T(x_c) = \Gamma_{Tc},\ n(x_w) = n_w,\ N(x_w) = N_w,\ T(x_w) = T_w. \tag{40}$$

Numerically calculated profiles are displayed in Fig. 12. They clearly demonstrate the losses due to the limiter and the fact that the radiation density of the impurities is localized in the scrape-off layer. To demonstrate existence according to eqs. (14) and relate it to the above analysis (Figs. 1, 3), phase space representations of these solutions are shown in Fig. 13. They prove the above existence analysis to be useful.

The maximum of the radiation is shifted towards the wall with increasing Γ_{Tc} and connection length L (this means increasing power input and decreasing limiter losses); see Figs. 15. These profiles will be used as the equilibrium state for the stability analysis in the next section.

4 Stability Analysis

We proceed to investigate the stability property of an existing and unique equilibrium state $\vec{y}_0(x)$ by means of a linear analysis. The expansion of the system of equations (9) at $\vec{y}_0$ results in

$$\left[\hat{A}(\vec{y}_0)\partial_t + \hat{E}\partial_x\right] \cdot \delta\vec{y} = \hat{J}_f(\vec{y}_0) \cdot \delta\vec{y} \tag{41}$$

with $\delta\vec{y} := \vec{y} - \vec{y}_0$. We look for *absolute instabilities*, and try to solve this equation with the ansatz $\delta\vec{y} \sim exp(\gamma t)$, which leads to

$$\partial_x \delta\vec{y} = \left[\hat{J}_f(\vec{y}_0) - \gamma\hat{A}(\vec{y}_0)\right] \cdot \delta\vec{y}. \tag{42}$$

To solve the eigenvalue problem (42), a BVP is formulated with boundary conditions which describe perturbations that may appear in the SOL: Positive eigenvalues $\gamma = const > 0$ with vanishing perturbed fluxes in the plasma center and a sufficiently small perturbation of the remaining quantities at the wall are assumed.

The reason for the excitation of the RTI is the existence of a part of the radiation profile which decreases with increasing temperature ($\partial Q_R/\partial T < 0$). The dependencies of the radiation discussed at the end of the foregoing section are also reflected in the location of the perturbations. This is shown in Figs. 14 for three different equilibrium states. The perturbations lead to the temporal development of the profiles which is shown in Figs. 15. The lowering of the temperature and the enhancement of the densities in the plasma edge result in a strong increase of the radiation. This shows that the RTI can lead to the formation of a strongly radiating, cold plasma belt.

However, only the onset of these unstable solutions can be described within the frame of the linear approach. But a small change of the phase space trajectory in the vicinity of quasi-singular points may lead to non-existence with regard to (15), which can be understood as bifurcation.

A numerical analysis, similar to that of this paper, has been presented in [13] applying a simple free-flight model for the neutral particles: $\Gamma_N = -v_N N$, where v_N is the velocity of the inward streaming neutrals coming from the wall; for $v_N = v_s\sqrt{k_i/2k_{cx}}$ this model is identical with the diffusion model of (5) for $T = const$, $R = 0$. Both models can be used to prove the sensitivity against the neutral gas description. Because we are concerned with effects localized in the scrape-off layer, where both models lead to similar neutral particle behaviour, we also obtain similar results.

5 Summary

A radial hydrodynamic model in planar approximation is used to investigate the radiative thermal instability in the scrape-off layer by applying a linear stability analysis of existing equilibrium states.

Before the stability analysis is presented, existence conditions for equilibrium states are investigated by analyzing trajectories in the 6-dimensional phase space S of particle densities, temperature and their respective fluxes. An equilibrium state is represented by a line in S with the spatial coordinate x as the curve parameter. In order to investigate existence conditions, the concept of quasi-singularity is introduced because physically allowed existence domains in S are limited by quasi-singular points. Therefore, it is necessary to analyze phase space portraits in the vicinity of quasi-singular points and look for conditions under which these portraits are changed when the parameters of the system are changed. When the phase space portrait gets restructured qualitatively bifurcation takes place. Whenever with changing x a quasi-singular region of the phase space is attained, a change of the parameters of the system may lead to bifurcation.

Quasi-singular regions are characterized by critical quantities: limits for the density, the temperature and the extension of the scrape-off layer. These quantities are evaluated for simplified cases of homogeneous temperature and plasma density, respectively, and in linear approximation. Analytical results are used wherever possible. The linearized solution shows bifurcation in its simplest form and indicates how the neutrals act: Neutral particles are shown to destabilize existing equilibrium states, i.e. they make existing domains smaller with increasing neutral density. These analysis is carried out for relevant physical tasks. How critical plasma densities in dependence of the temperature can be calculated and how the different loss mechanisms contribute, was shown in ref. [8]. Here we discuss only one simple example, which shows that ionization loss over the whole scrape-off layer is negligible, and that for low temperatures the radiation loss becomes comparable to the energy loss due to the limiter. For the self-consistent numerical analysis a boundary value problem is formulated whose phase tracectories attain quasi-singular points. The numerically calculated equilibrium profiles clearly demonstrate the losses due to the limiter and the fact that the radiation density of the impurities is localized in the scrape-off layer with a maximum which is shifted towards the wall with increasing energy influx and connection length.

This numerically calculated equilibrium state is investigated with regard to the radiative thermal instability. To solve this eigenvalue problem, a suitably chosen boundary value problem is formulated which describes perturbations of the densities, the temperature and their respective fluxes that may appear in the scrape-off layer. It is shown that absolutely unstable solutions may exist. This has also been shown for other equilibrium states than that one used here, for instance for the case that heating is neglected [8]. The reason for the excitation of the radiative thermal instability is the branch with negative

characteristic in the radiation rate, i.e. $\partial Q_R/\partial T < 0$. The latter is in fact a necessary condition for the occurance of the instability. The dependencies of the radiation on the energy influx and the connections length, mentioned above, are also reflected in the location of the perturbations which are also shifted towards the wall with increasing energy influx and connection length. These absolutely unstable perturbations can lead to the formation of a strongly radiating, cold, detached plasma belt. Moreover, they have an effect on the parameters of the boundary value problem. These parameters may be changed until bifurcation occurs. Thus bifurcation is revealed here as the essential mechanism that disrupt the equilibrium. Bifurcation may also lead to transitions between different eqilibrium states, e.g. L to H mode bifurcation [16].

Furthermore, bifurcation (branching, hysteresis effects) of the electron temperature in a stable plasma can be caused by the nonlinear temperature dependence of the impurity radiation in the SOL [14] or the ionization losses in the high recycling layer in the front of the divertor target plates [15]. Bifurcation also occurs, for instance, in magnetic field structures of fusions plasmas. From a more general point of view, this paper may be seen as a fundamental treatment of *bifurcation physics* [17] in SOL modelling.

References

[1] Wesson, J.A., Gill, R.D., Hugon, M., et al., Nucl. Fusion 29(1989)641

[2] Stäbler, A., McCormick, K., Mertens, V., et al, Nucl. Fusion 32(1992)1557

[3] Drake, J.F., Phys. Fluids 30(1987)2429

[4] Roy Choudbury, S., Kaw, P.K., Phys. Fluids B1(1989)1646

[5] Abramov, V.A., Lisitsa, V.S., Morozov, D.Kh, Contrib. Plasma Phys. 32(1992)400

[6] Bachmann, P., Morozov, D.Kh., Sünder, D., Contrib. Plasma Phys. 32(1992)395

[7] Abramov, V.A., Bachmann, P., Morozov, D.Kh., Sünder, D., 20th EPS, Lisboa 1993. Contributed Papers II-823

[8] Abramov, V.A., Bachmann, P., Morozov, D.Kh., Sünder, D., Contrib. Plasma Phys. 34(1994)271

[9] Walter, W., Differential and Integral Inequalities, Springer-Verlag, Berlin 1970

[10] Hairer, E., Noersett, S.P., Wanner, G., Solving Ordinary Differential Equations I, Springer-Verlag, Berlin 1987

[11] Neimark, Yu.I., Landa, P.S., Stochastic and Chaotic Oscillations, Kluwer Academic Publishers, Dorfrecht 1992

[12] Ebeling, W., Engel, H., Herzel, H., Selbstorganisation in der Zeit, Akademie-Verlag Berlin 1990

[13] Bachmann, P., Sünder, D., 21st EPS, Montpellier 1994, Contributed Papers

[14] Capes, H., Ghendrih, Ph., Samain, A., Phys. Fluids B4 (1992) 1287

[15] Sünder, D., Wobig ,H., 20th EPS, Lisboa 1993, Contrib. Papers II-819

[16] Carreras, B.A., Diamond, P.H., Liang, Y.-M., et al., Plasma Phys. Control Fusion 36(1994)A93

[17] Itoh, K., Plasma Phys. Control. Fusion 36(1994)A307

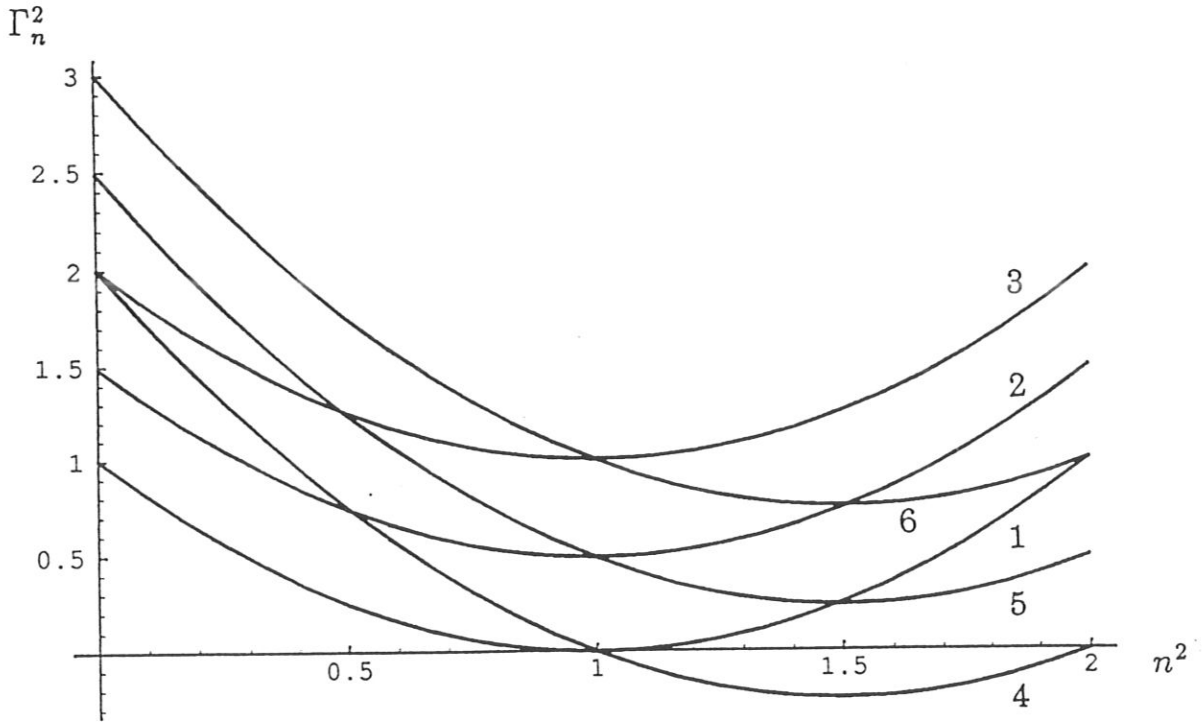

Fig. 1
Phase space representation for the domain I ($x < 0$) : Γ_n^2 as a function of n^2 for different parameters (μ, Γ_{nc}) : $1-(1,0)$, $2-(1,0.5)$, $3-(1,1)$, $4-(1.5,0)$, $5-(1.5,0.5)$, $6-(1.5,1)$ with dimensionless quantities (21).

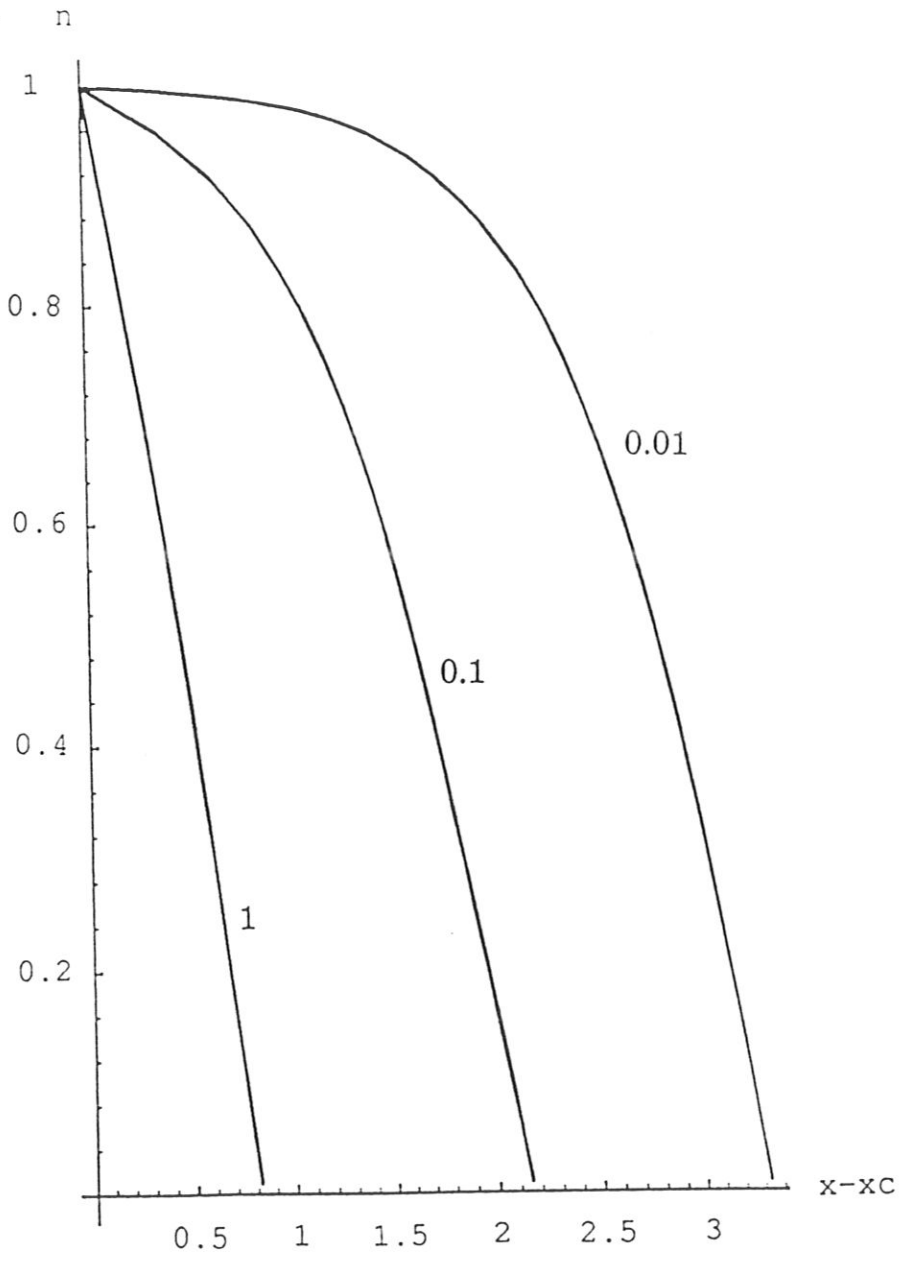

Fig. 2
Density profiles for the domain I ($x < 0$) for $\mu = 1$ and different Γ_{nc} values with dimensionless quantities (21).

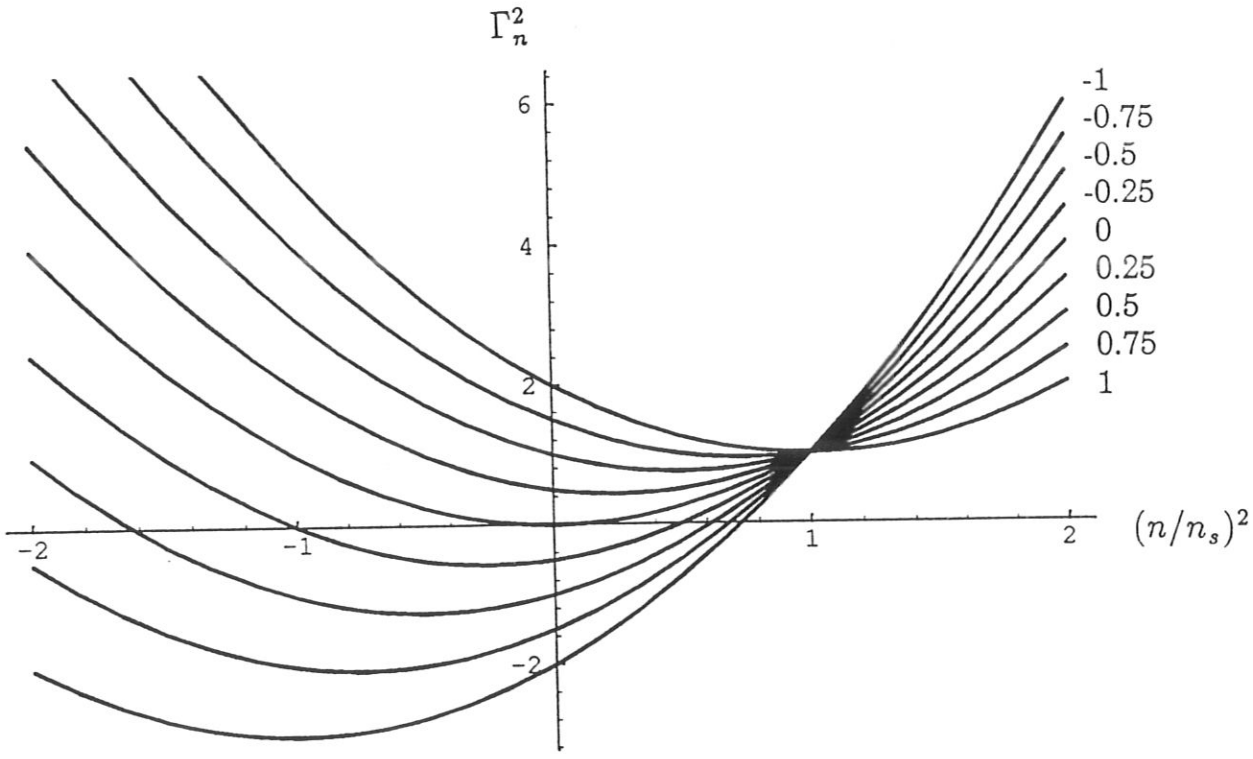

Fig. 3
Phase space representation for the domain II ($x > 0$): Γ_n^2 as a function of $(n/n_s)^2$ for $\Gamma_{ns} = 1$ and $\mu = -1...1$ with dimensionless quantities (21).

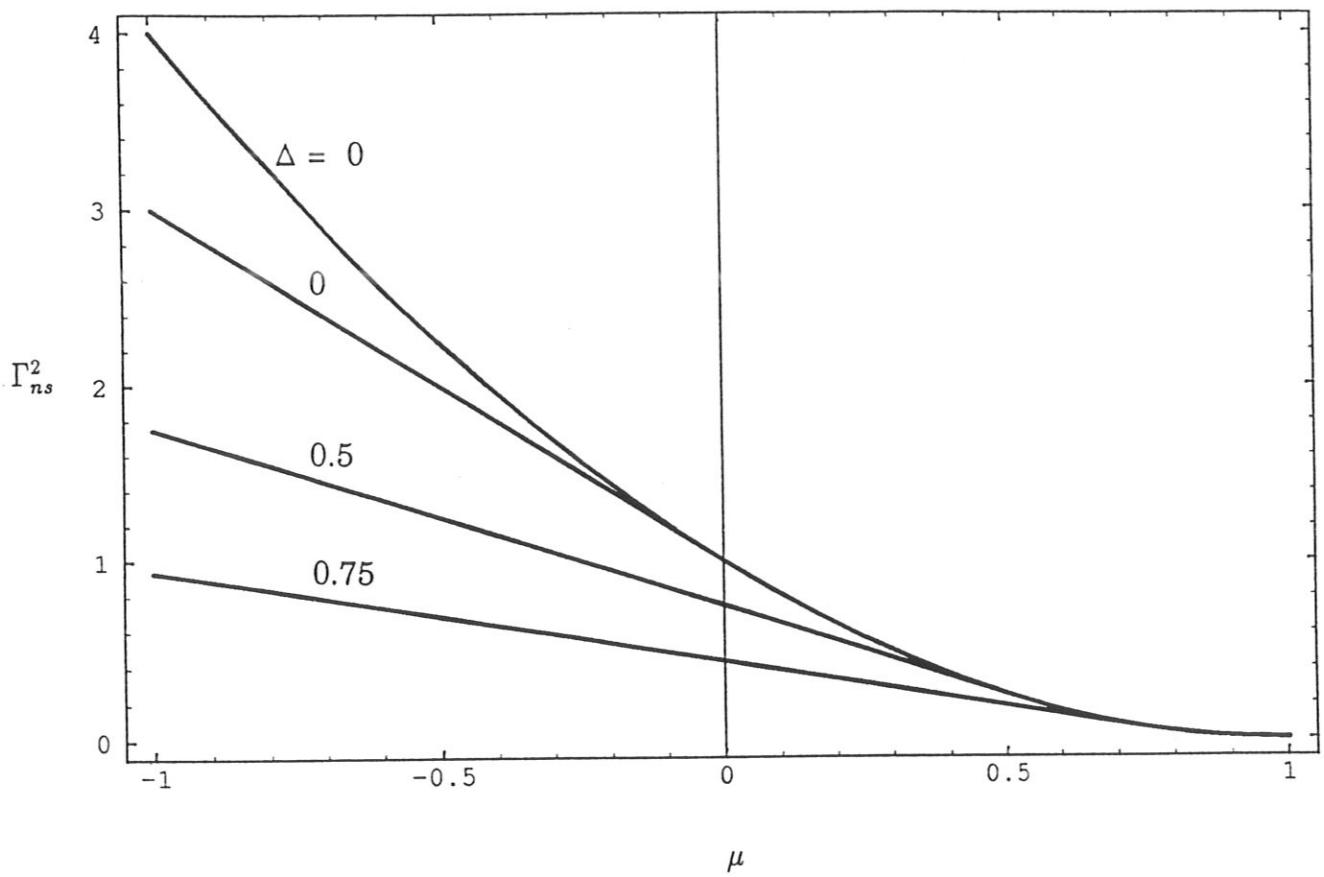

Fig. 4
Existence diagrams for the domain II with the bifurcation lines $\Delta(\mu, \Gamma^2_{ns}) = 0$, $n_1^2 = 0,\ 0.5,\ 0.75$ with dimensionless quantities (21). Equilibrium states may exist above the curves.

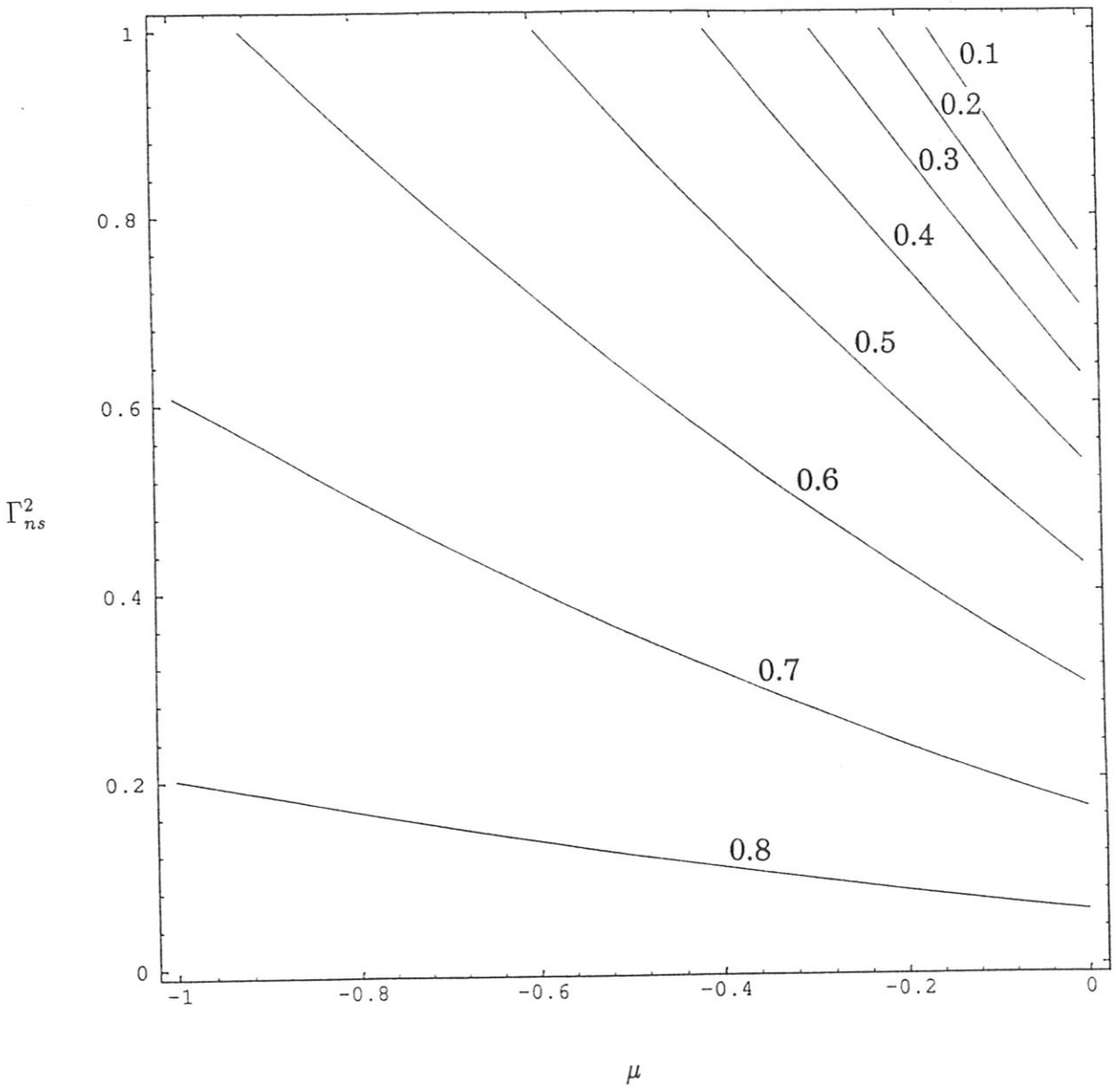

Fig. 5
Existence diagrams for the domain II with x_{10} as the parameter with dimensionless quantities (21).

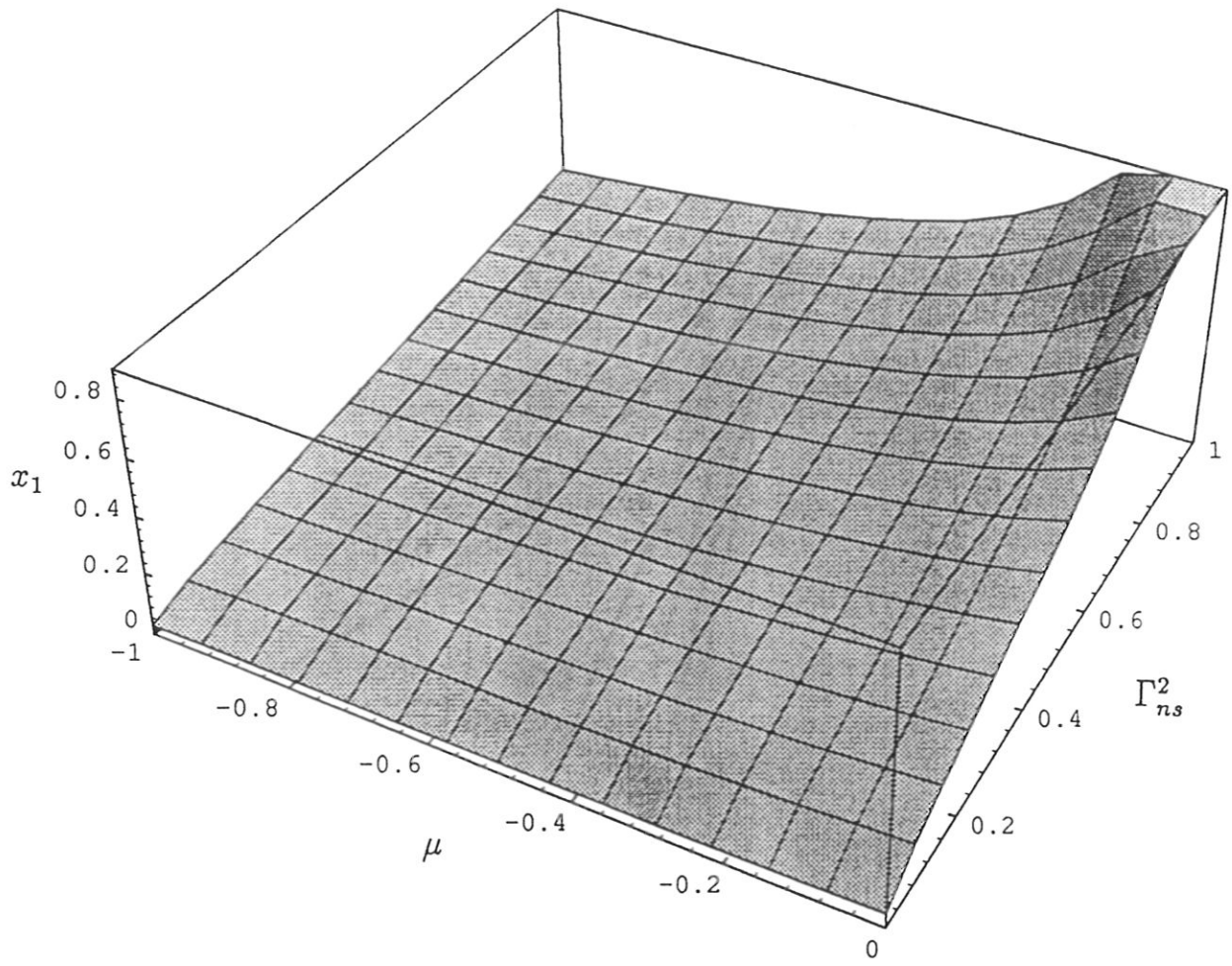

Fig. 6
x_1 as a function of μ, Γ^2_{ns} with bifurcation surface with dimensionless quantities (21).

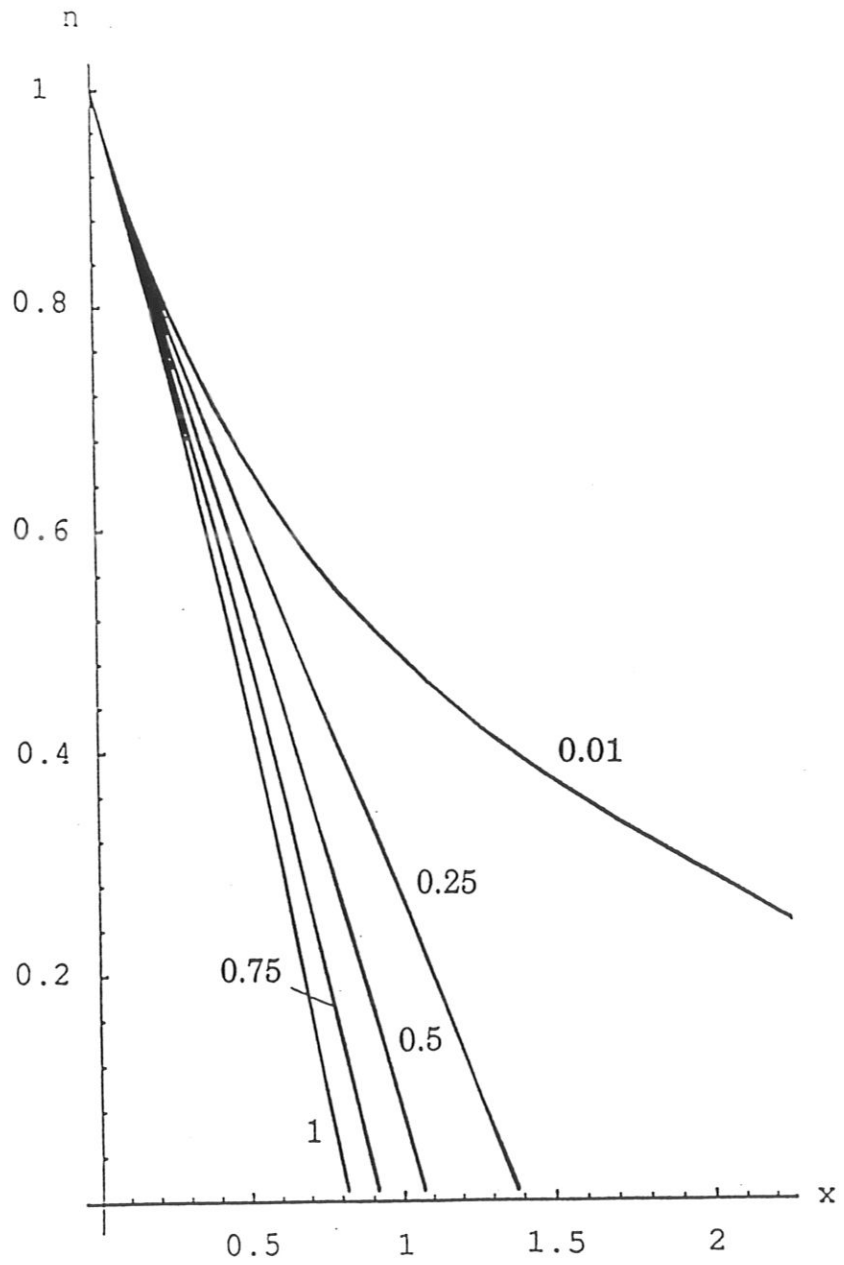

Fig. 7
Density profiles for the domain II ($x > 0$) for $\Gamma_{ns} = 1$ and different μ values with dimensionless quantities (21).

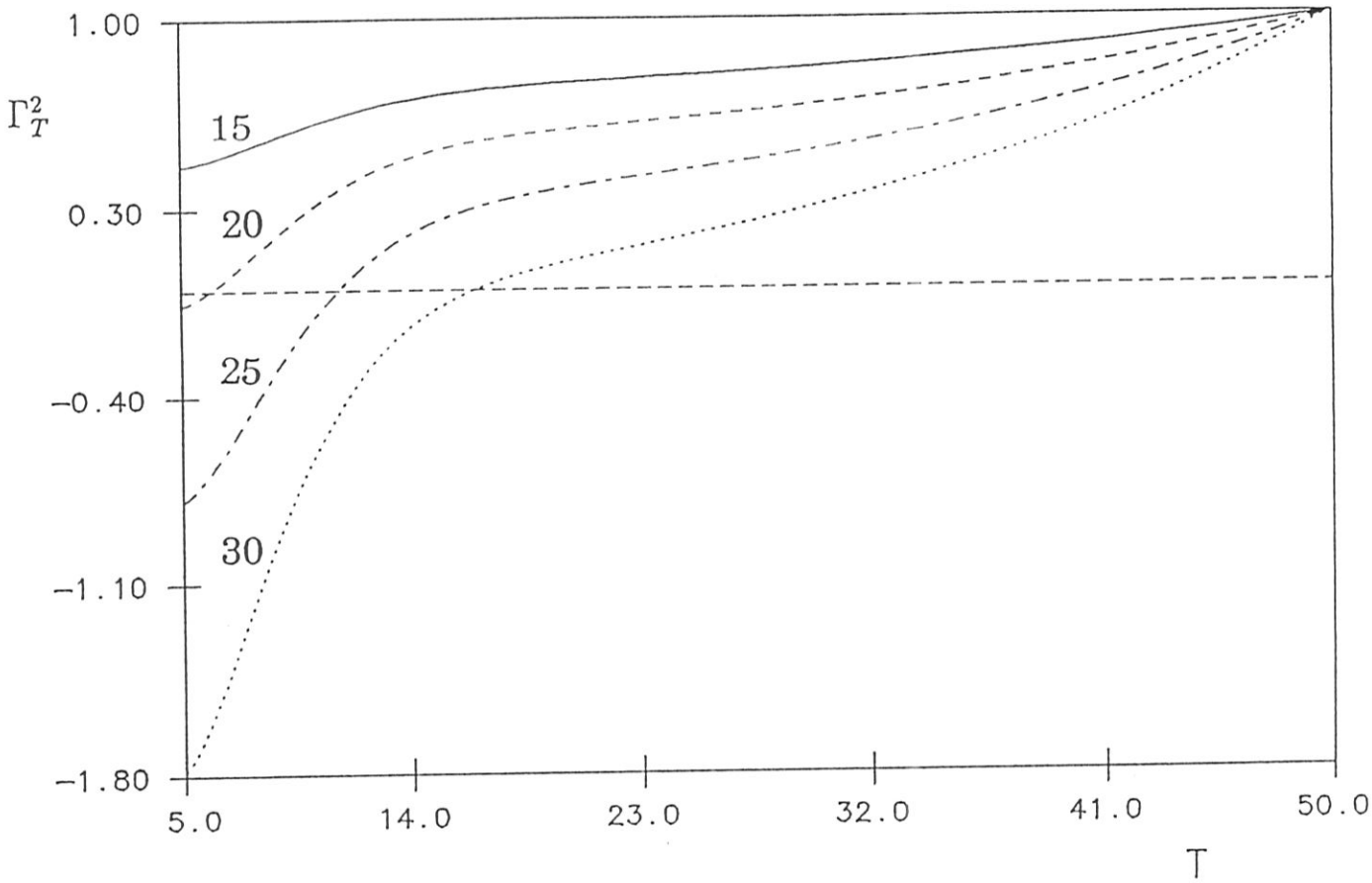

Fig. 8a
Γ_T^2 as a function of T with n as parameter for $N_s = 10^{-2}$ with dimensionless quantities (32).

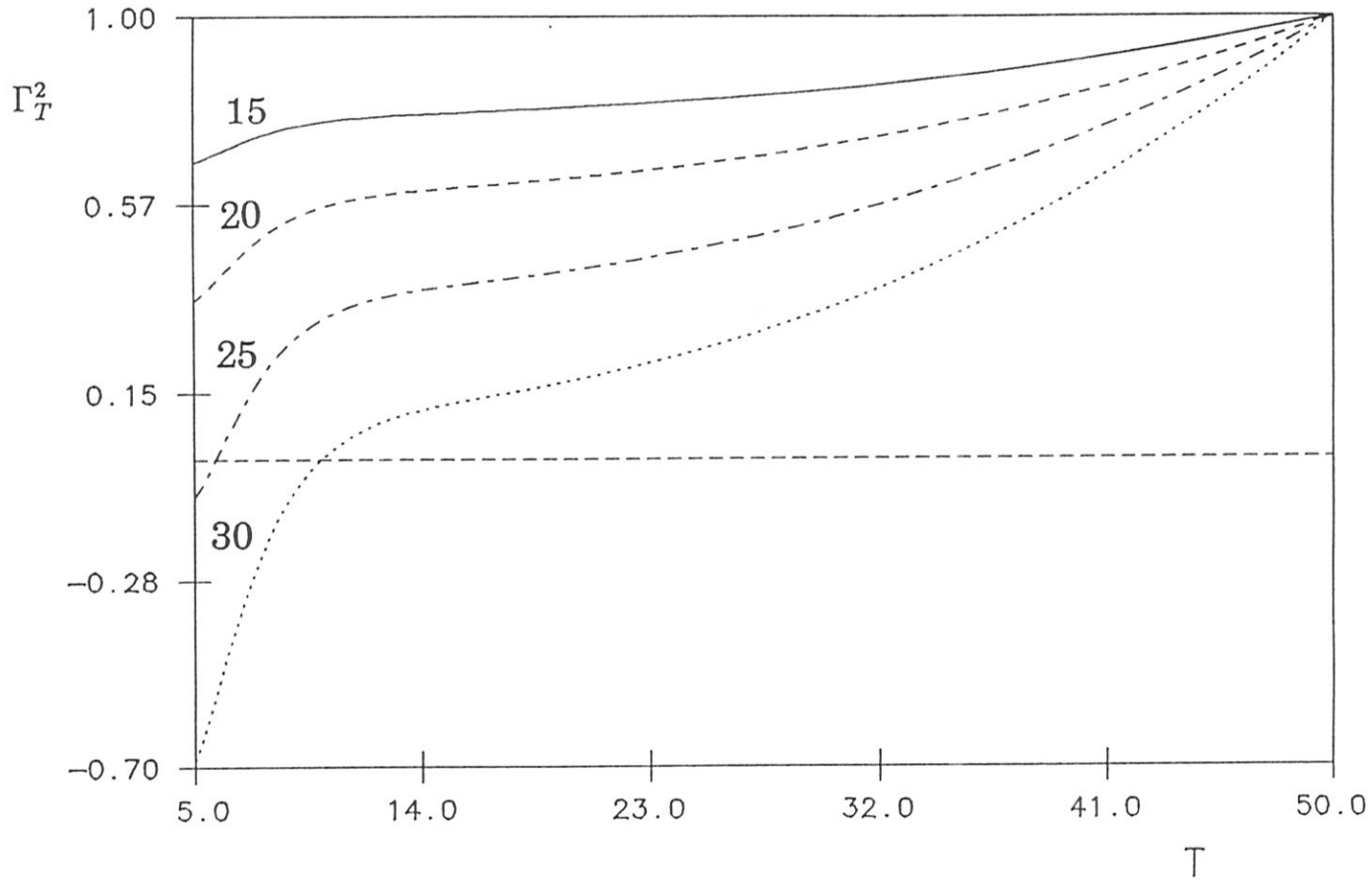

Fig. 8b
Γ_T^2 as a function of T with n as parameter for $N_s = 10^{-4}$ with dimensionless quantities (32).

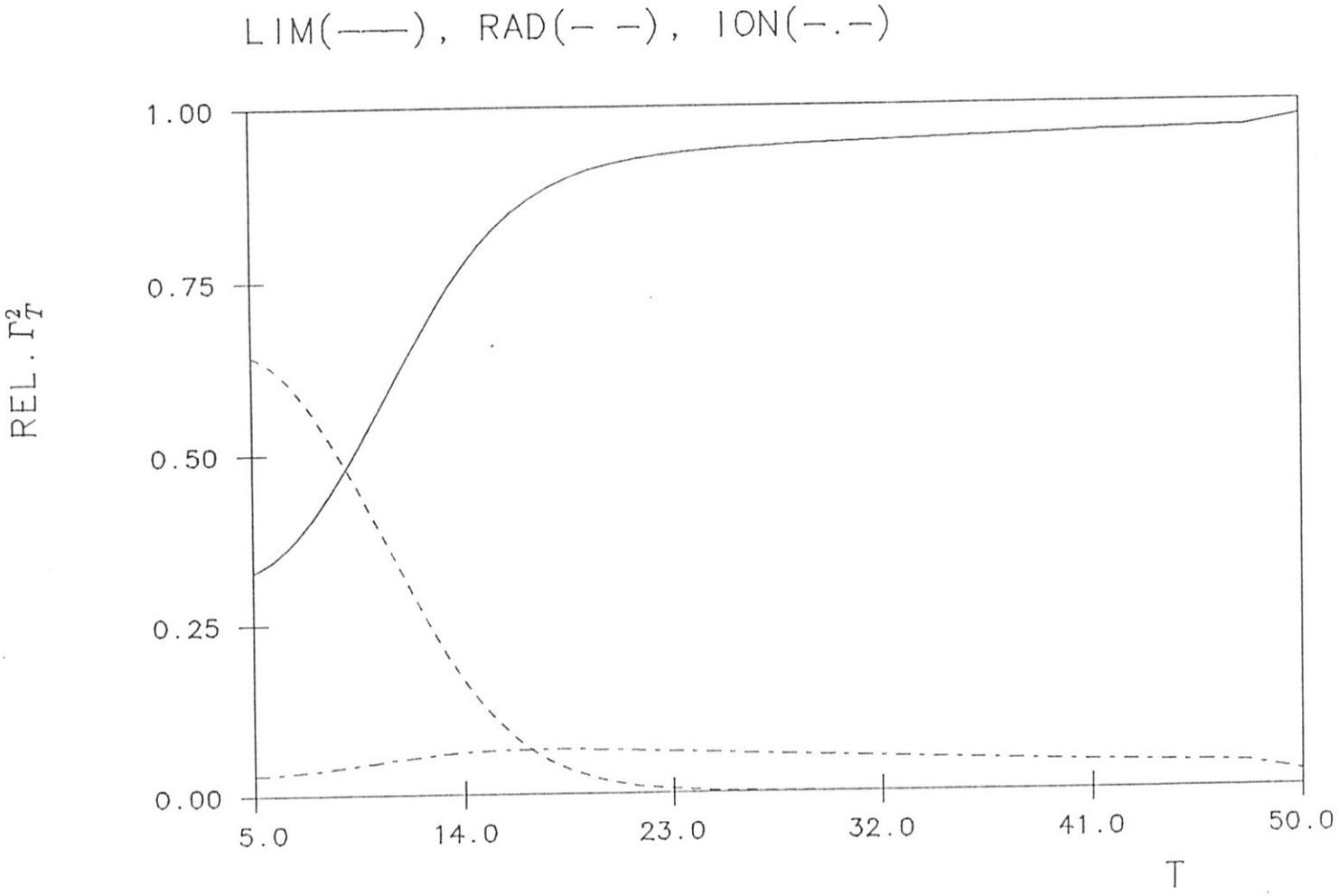

Fig. 9
Contribution of the different energy loss processes for $L = 3500,\ n = 30,\ N_s = 10^{-2}$ with dimensionless quantities (32).

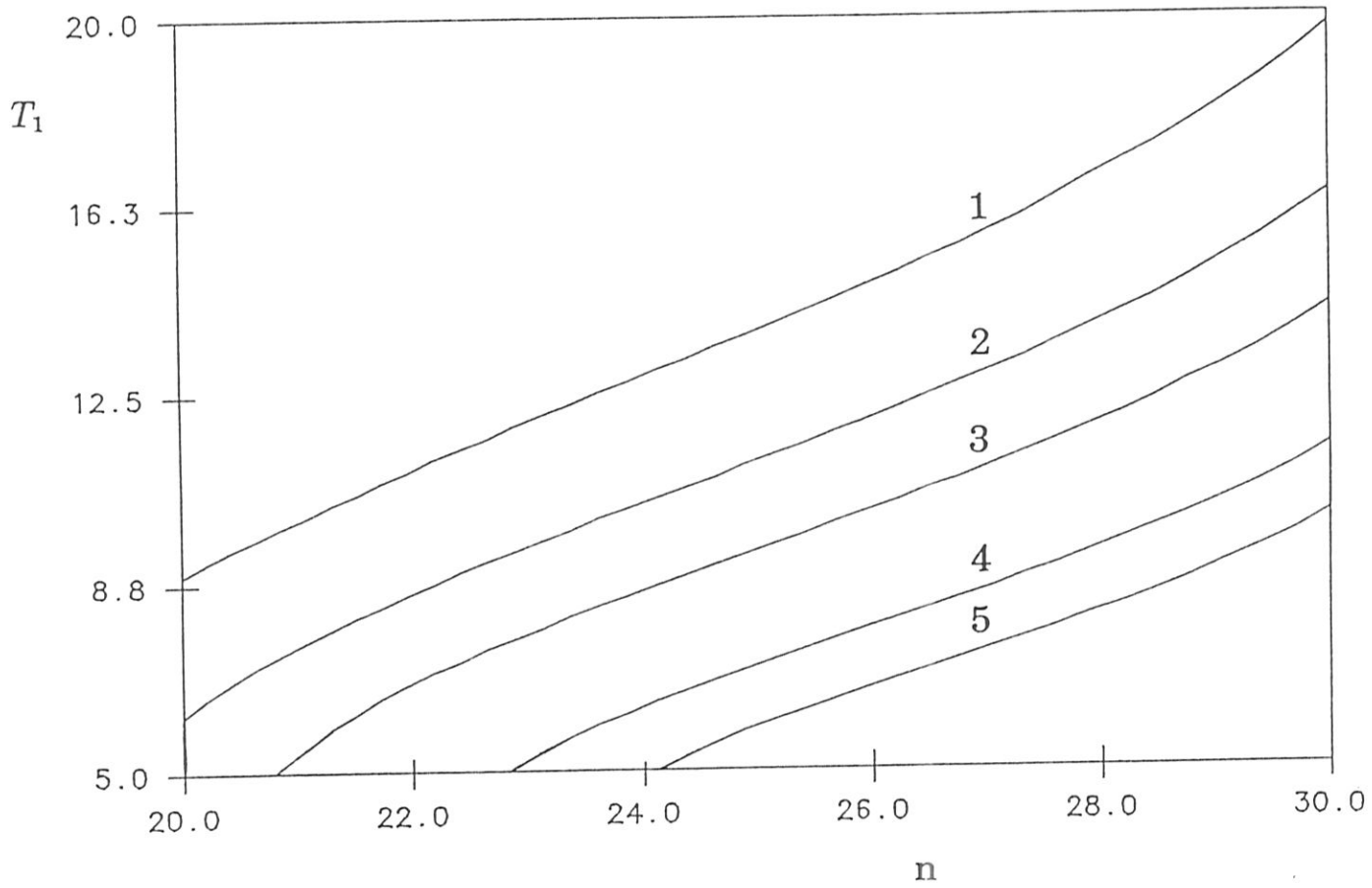

Fig. 10
Existence diagram (n, T). Equilibrium states may exist above the curves $T_1(n)$ for $N_s = 2 \times 10^{-2}$ (1), 10^{-2} (2), 5×10^{-3} (3), 10^{-3} (4), 10^{-4} (5) with dimensionless quantities (32).

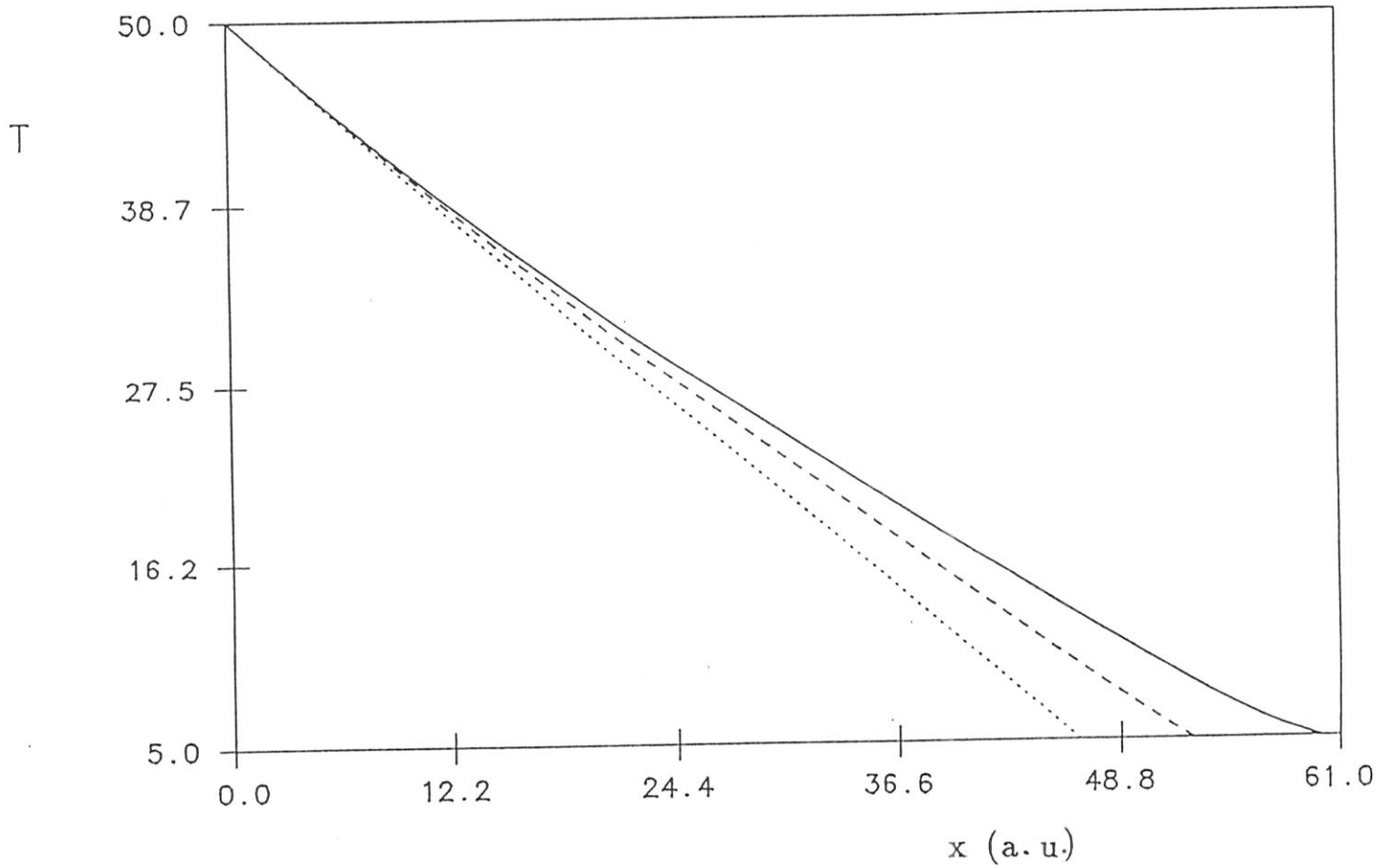

Fig. 11
Temperature profiles for $N_s = 10^{-4}$ and $n = 23$ (–), 19 (- -) and 10(...) with dimensionless quantities (32).

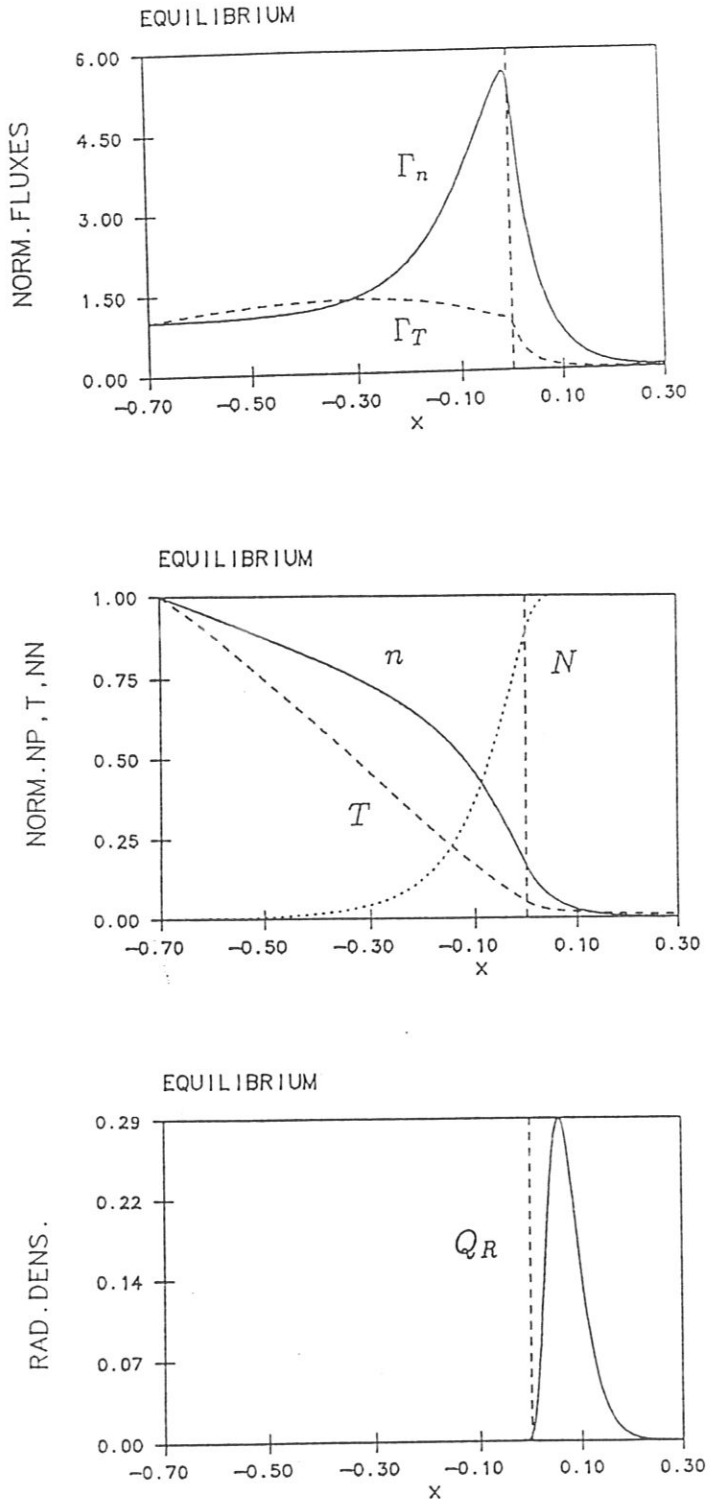

Fig. 12
Profiles of particle flux Γ_n [$10^{17} s^{-1} cm^{-2}$], energy flux Γ_T [2 $W cm^{-2}$], temperature T [570 eV], plasma density n [8.2 $10^{13} cm^{-3}$], neutral particle density N [$10^{10} cm^{-3}$], radiation density Q_R [$W cm^{-3}$], x [0.5 m], $T_w = 5$ eV, $n_w = 10^8$ cm^{-3}. $(n_c/n) = 0.01, D = 10^4$ $cm^2 s^{-1}, L = 10$ m

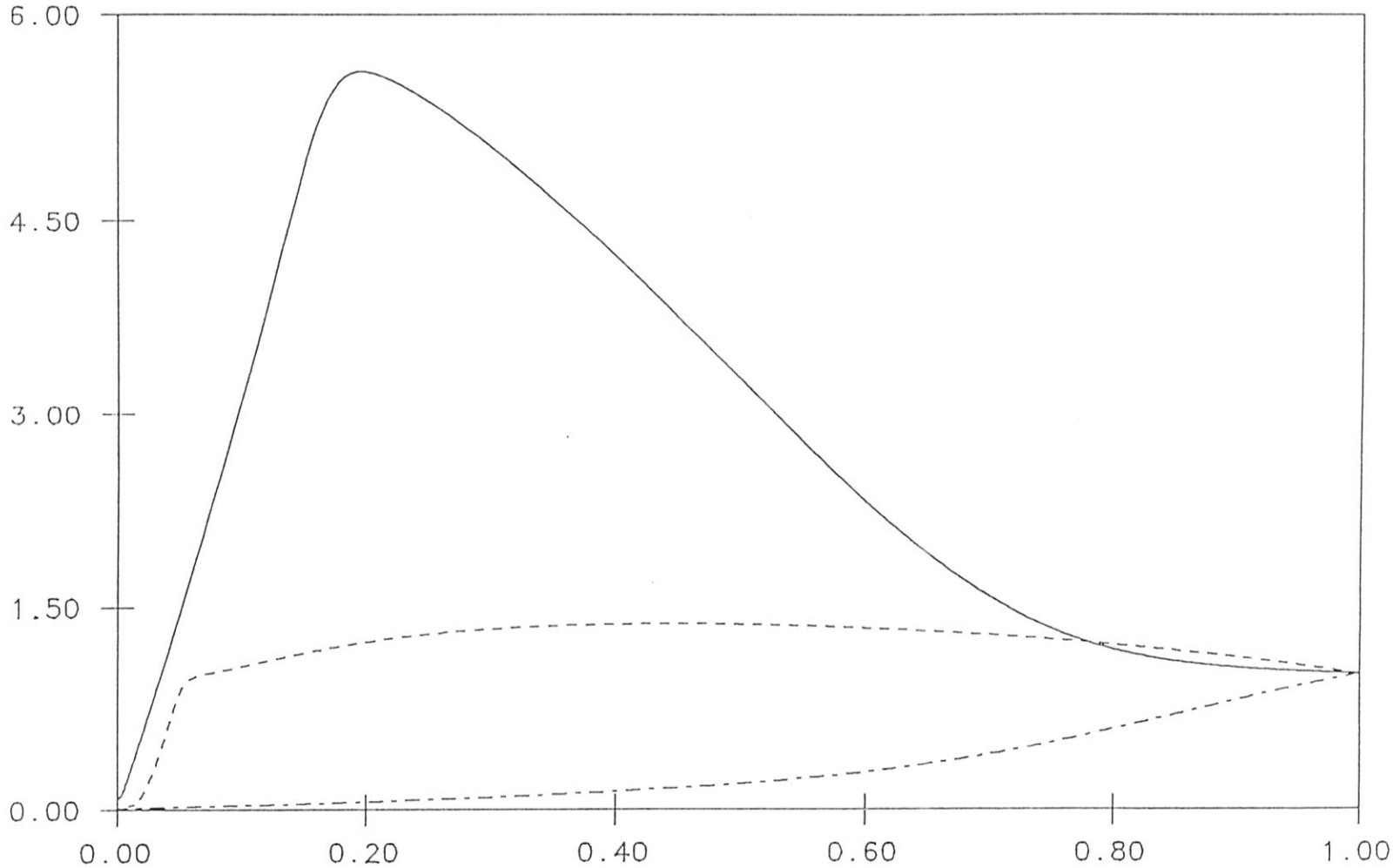

Fig. 13
Phase space representations (n, Γ_n) (—), (T, Γ_T) (−−), (n, T) (−.−) for Fig. 12.

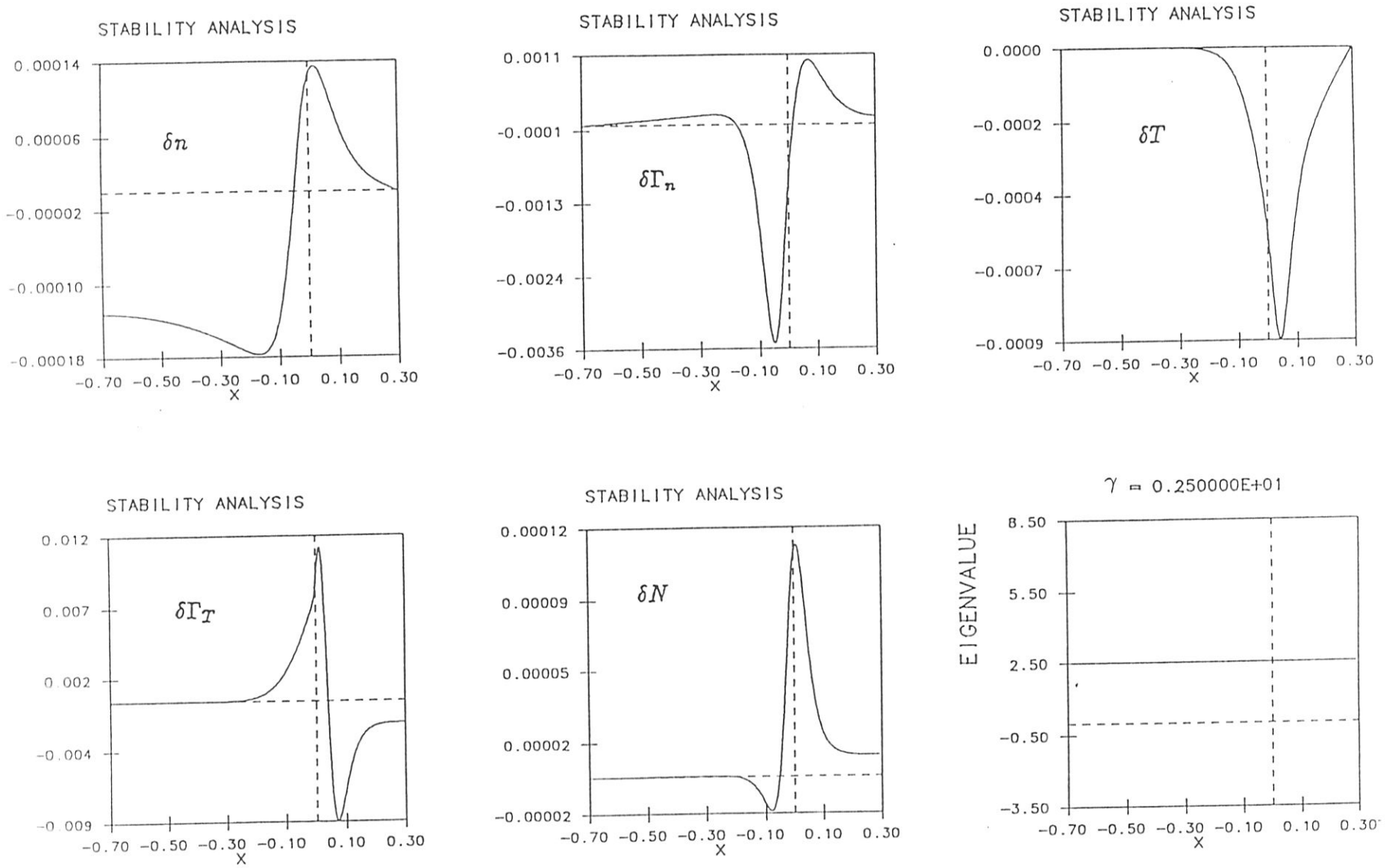

Fig. 14a
Perturbation of plasma density (δn), particle flux ($\delta\Gamma_n$), temperature (δT), energy flux ($\delta\Gamma_T$), neutral particle density (δN) profiles and growth rate (γ) (in a.u.) for the eqilibrium state with $\Gamma_{nc} = 10^{17} s^{-1} cm^{-2}$, $n_w = 10^8\ cm^{-3}$, $N_w = 10^{10}\ cm^{-3}$, $T_w = 5\ eV$ and $\Gamma_{Tc} = 2\ W cm^{-2}$, $L = 10\ m$; x [0.5 m].

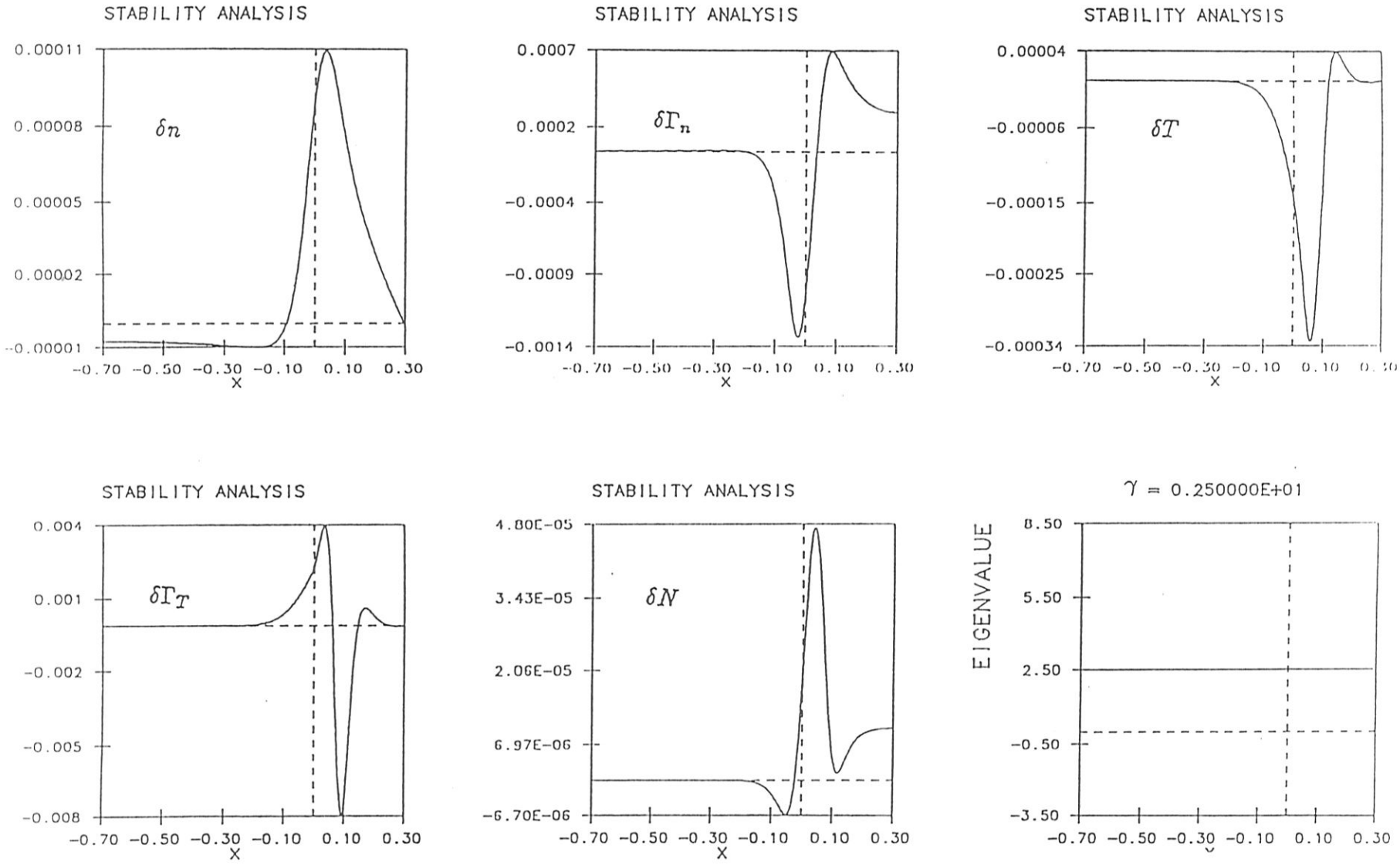

Fig. 14b

Perturbation of plasma density (δn), particle flux ($\delta\Gamma_n$), temperature (δT), energy flux ($\delta\Gamma_T$), neutral particle density (δN) profiles and growth rate (γ) (in a.u.) for the eqilibrium state with $\Gamma_{nc} = 10^{17} s^{-1} cm^{-2}$, $n_w = 10^8\ cm^{-3}$, $N_w = 10^{10}\ cm^{-3}$, $T_w = 5\ eV$ and $\Gamma_{Tc} = 2\ W cm^{-2}$, $L = 40\ m$; x [0.5 m].

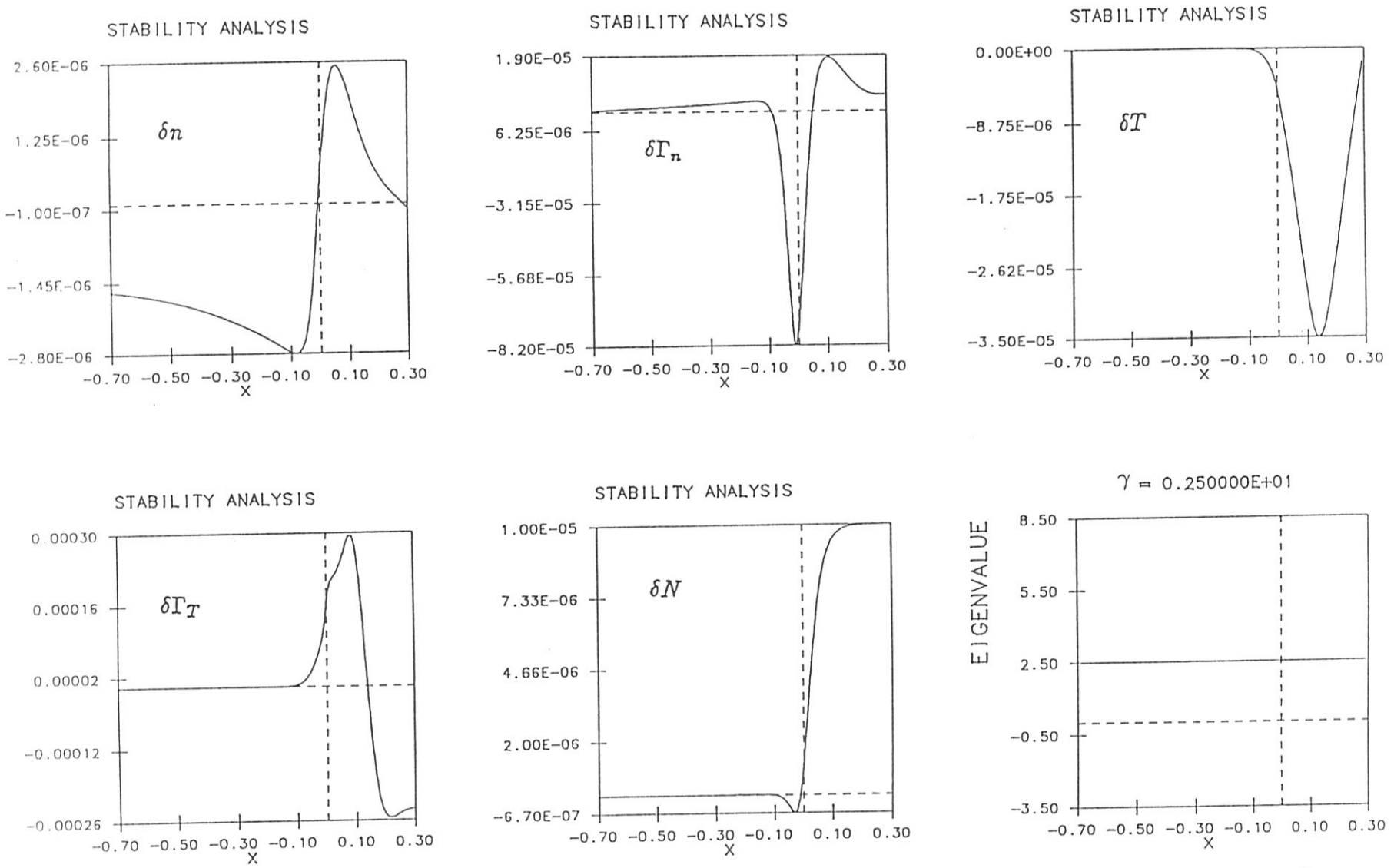

Fig. 14c

Perturbation of plasma density (δn), particle flux ($\delta\Gamma_n$), temperature (δT), energy flux ($\delta\Gamma_T$), neutral particle density (δN) profiles and growth rate (γ) (in a.u.) for the eqilibrium state with $\Gamma_{nc} = 10^{17} s^{-1} cm^{-2}$, $n_w = 10^8\ cm^{-3}$, $N_w = 10^{10}\ cm^{-3}$, $T_w = 5\ eV$ and $\Gamma_{Tc} = 4\ W cm^{-2}$, $L = 10\ m; x\ [0.5\ m]$.

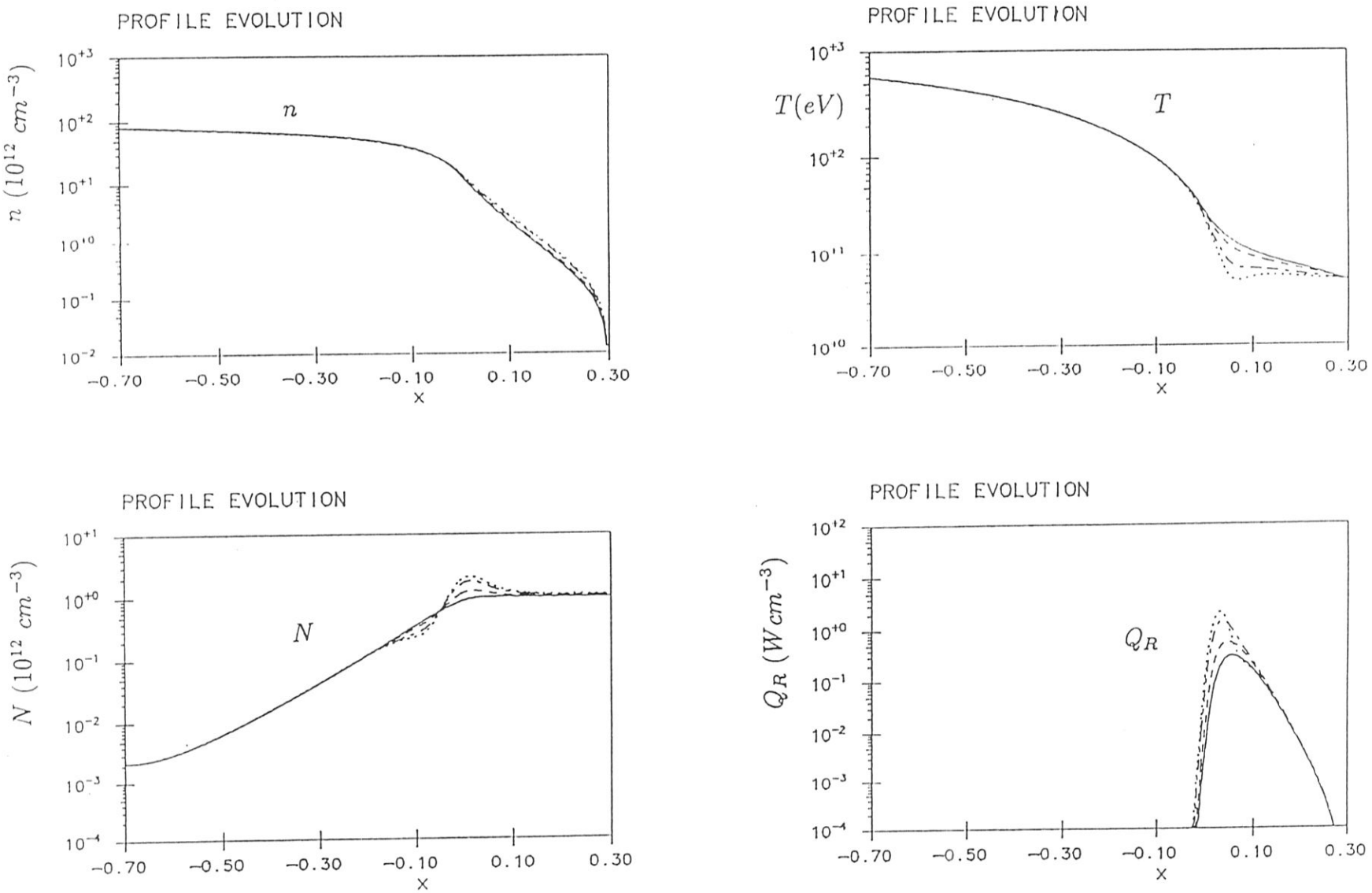

Fig. 15a
Profile evolution of the plasma density (n), temperature (T), neutral particle density (N) and radiation density (Q_R) for $\gamma t =$ 0 (—), 4 (−−), 5 (−.−), 5.3 (...), $\gamma = 25\ s^{-1}$ for parameters of Fig. 14a.

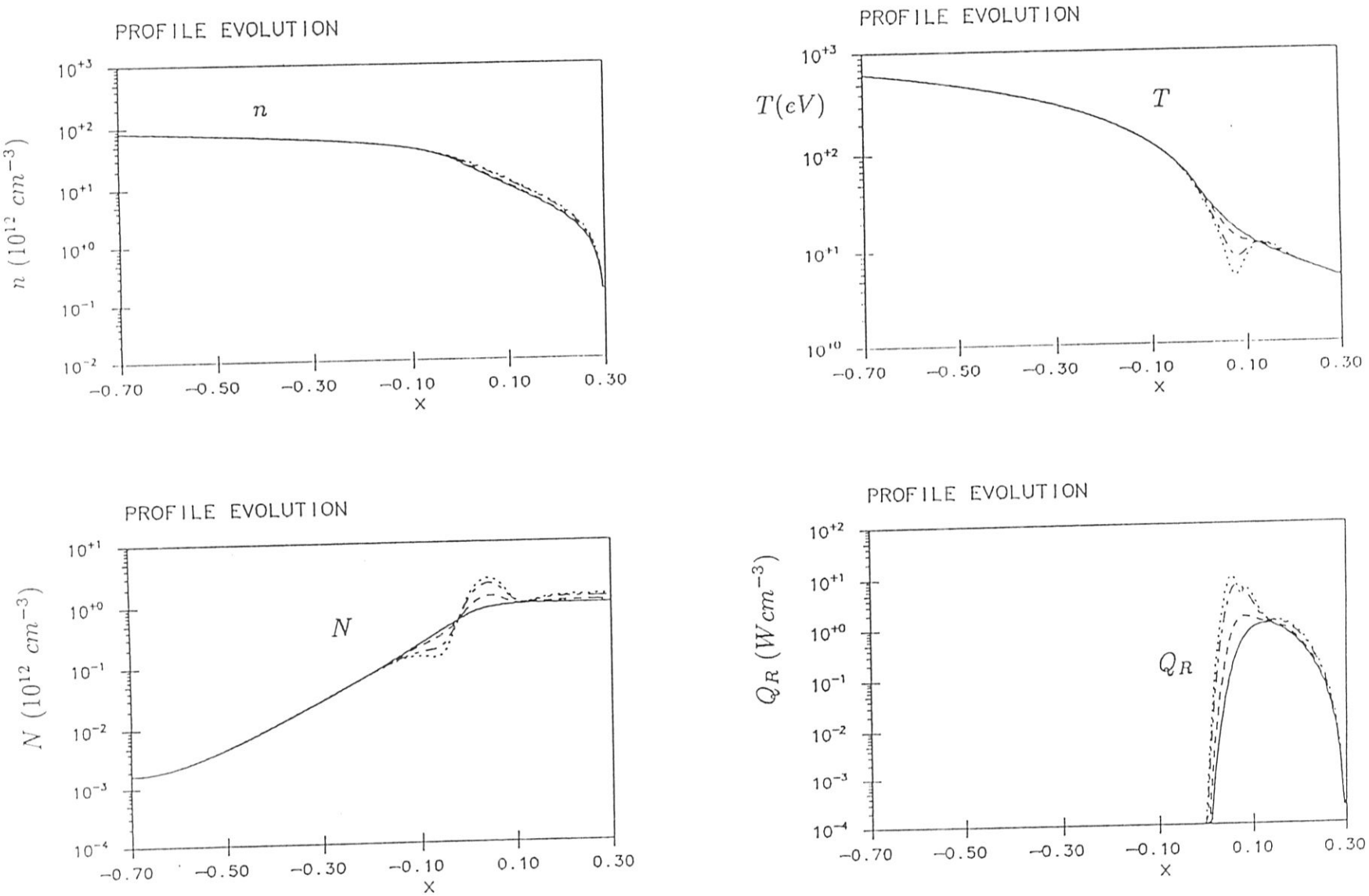

Fig. 15b
Profile evolution of the plasma density (n), temperature (T), neutral particle density (N) and radiation density (Q_R) for $\gamma t =$ 0 (—), 4 (−−), 5 (−.−), 5.3 (...), $\gamma = 25\ s^{-1}$ for parameters of Fig. 14b.

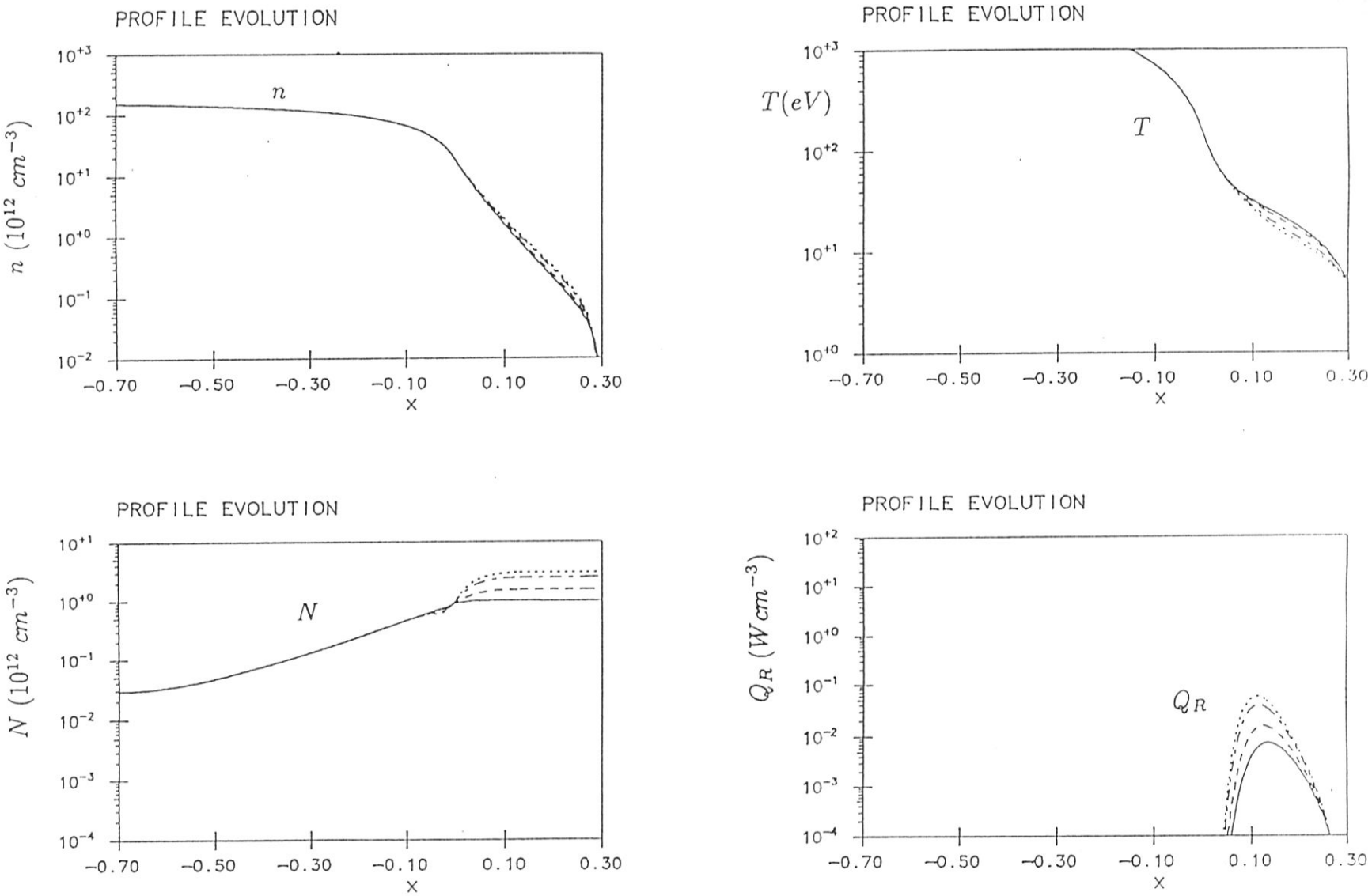

Fig. 15c
Profile evolution of the plasma density (n), temperature (T), neutral particle density (N) and radiation density (Q_R) for $\gamma t =$ 0 (—), 4 (−−), 5 (−.−), 5.3 (...), $\gamma = 25\ s^{-1}$ for parameters of Fig. 14c.